Supporting Information: Efficient Prediction of Mole Fraction Related Vibrational Frequency Shifts

Jan Blasius,[†] Katrin Drysch,[†] Frank Hendrik Pilz,[‡] Tom Frömbgen,[†,¶] Patrycja Kielb,[§,‡] and Barbara Kirchner[*,†]

†*Mulliken Center for Theoretical Chemistry, Clausius Institute of Physical and Theoretical Chemistry, University of Bonn, Beringstraße 4–6, D-53115 Bonn, Germany*

‡*Clausius Institute of Physical and Theoretical Chemistry, University of Bonn, Wegelerstraße 12, D-53115 Bonn, Germany*

¶*Max-Planck-Institut für Chemische Energiekonversion, Stiftstrasse 34-36, D-45470 Mülheim an der Ruhr, Germany*

§*Transdisciplinary Research Area "Building Blocks of Matter and Fundamental Interactions" (TRA Matter), University of Bonn, Bonn, Germany*

E-mail: kirchner@thch.uni-bonn.de

Contents

1 Methods

1.1 QCE Method or Cluster-Weighting

The theory of the quantum cluster equilibrium method (QCE) and its extension to binary systems (bQCE) has been extensively described in several earlier works.[1–6] In general, this method considers the liquid phase as an ensemble of interacting molecular clusters. The cluster distribution of this ensemble is obtained through expressions of statistical thermodynamics and by introducing extensions in the cluster partition functions. Based on the obtained cluster populations and the system's total partition function, the thermodynamic properties of the system are accessible in a selected temperature range. Herein we will only provide an overview of the basic aspects of QCE and bQCE and discuss the most recent modifications of the partition functions.

Within the QCE method, the cluster ensemble is considered to be in thermodynamic equilibrium. This equilibrium can be expressed as

$$\mathrm{C}_1 \rightleftharpoons \frac{\mathrm{C}_2}{i(2)} \rightleftharpoons \frac{\mathrm{C}_3}{i(3)} \rightleftharpoons \cdots \rightleftharpoons \frac{\mathrm{C}_\wp}{i(\wp)} \tag{1}$$

for a neat substance and extends to

$$i(\wp)\mathrm{C}_1 + j(\wp)\mathrm{C}_2 \rightleftharpoons \mathrm{C}_\wp \tag{2}$$

for a binary mixture. Therein, a cluster $\mathrm{C}_\wp$ is formed by $i(\wp)$ and $j(\wp)$ monomers of the components C_1 and C_2. Assuming independent clusters and independent translational, vibrational, rotational and electronic degrees of freedom, the system's total partition function is given by

$$Q^{\mathrm{tot}}(\{N_\wp\}, V, T) = \prod_{\wp=1}^{N} \frac{1}{N_\wp!}[q_\wp^{\mathrm{tot}}(V,T)]^{N_\wp}, \tag{3}$$

with

$$q_{\wp}^{\mathrm{tot}}(V,T) = q_{\wp}^{\mathrm{trans}}(V,T) q_{\wp}^{\mathrm{vib}}(T) q_{\wp}^{\mathrm{rot}}(T) q_{\wp}^{\mathrm{elec}}(V,T). \tag{4}$$

Therein, $\{N_{\wp}\}$ is the full set of cluster populations $N_{\wp}$, T and V are the temperature and volume, respectively, and $q_{\wp}^{\mathrm{tot}}$ is the partition function of a single cluster $\mathrm{C}_{\wp}$. The translational, vibrational and rotational partition functions, $q_{\wp}^{\mathrm{trans}}$, $q_{\wp}^{\mathrm{vib}}$ and $q_{\wp}^{\mathrm{rot}}$ are based on standard expressions for the particle in a box, the harmonic oscillator and the rigid rotor, respectively.[7,8] The electronic partition function $q_{\wp}^{\mathrm{elec}}$ is calculated from the referenced binding energy $\varepsilon_{\wp}^{\mathrm{elec}}$ of the respective cluster.

Up to this point, the system consists of non-interacting and point-shaped particles. However, to achieve a proper description of the liquid phase, inter-cluster interactions as well as the finite cluster volumes need to be considered. The finite cluster volumes are taken into account by introducing an exclusion volume

$$V^{\mathrm{excl}} = b_{\mathrm{xv}} \sum_{\wp=1}^{N} N_{\wp} v_{\wp} \tag{5}$$

which is subtracted from the phase volume V in the translational partition function. The empirical exclusion volume parameter b_{xv} scales the cluster volumes $v_{\wp}$, which are known to be sensitive with respect to the choice of the atomic radii. A recent extension[9] of the QCE theory introduced a linear temperature dependence of b_{xv}:

$$b_{\mathrm{xv}}(T) = T \cdot \beta_{\mathrm{xv}} + b_{\mathrm{xv}}^{0}. \tag{6}$$

Here, β_{xv} and b_{xv}^{0} are the exclusion volume expansion coefficient and the base of the intercept, respectively.

The inter-cluster interactions are taken into account by introducing a volume dependent mean-field-like attractive energy term in the electronic partition function, which therefore

reads as

$$q_{\wp}^{\mathrm{elec}}(V,T) = \exp\left(-\frac{\epsilon_{\wp}^{\mathrm{elec}} - [i(\wp) + j(\wp)]\frac{a_{\mathrm{mf}}}{V}}{k_{\mathrm{B}}T}\right). \tag{7}$$

Therein, the empirical mean-field parameter a_{mf} scales the strength of the inter-cluster interactions and k_{B} is the Boltzmann constant.

Another recently introduced modification[10] targets the vibrational partition function, whose combination with the rotational partition function is usually referred to as the rigid-rotor–harmonic-oscillator approximation. However, since the vibrational partition function diverges for $\nu_i \longrightarrow 0$, with ν_i being a vibrational mode,[11] the modified rigid-rotor–harmonic-oscillator (mRRHO) approximation introduces the vibrational partition function as

$$q_i^{\mathrm{vib}} = \prod_{\nu_i}^{N_i^{\mathrm{vib}}} \left(q_{\mathrm{HO}}^{\mathrm{vib}}(\nu_i)\right)^{f(\nu_i)} \cdot \left(q_{\mathrm{HR}}^{\mathrm{vib}}(\nu_i)\right)^{1-f(\nu_i)}. \tag{8}$$

Within this modified vibrational partition function, $q_{\mathrm{HR}}^{\mathrm{vib}}$ is the partition function of the hindered rotor

$$q_{\mathrm{HR}}^{\mathrm{vib}}(\nu_i) = \sqrt{\frac{2\mu'(\nu_i)}{\pi\hbar^2\beta}} \qquad \text{with} \quad \mu'(\nu_i) = \frac{\mu(\nu_i)\bar{I}}{\mu(\nu_i) + \bar{I}} \quad \text{and} \quad \mu(\nu_i) = \frac{\hbar}{4\pi\nu_i} \tag{9}$$

and $q_{\mathrm{HO}}^{\mathrm{vib}}$ is the partition function of the harmonic oscillator. Therein, $\bar{I}$ corresponds to the average moment of inertia of the cluster, μ is the moment of inertia corresponding to the normal mode and $\hbar$ is the reduced Planck constant. The Chai–Head-Gordon damping function[3]

$$f(\nu_i) = \left(1 + \left(\frac{\nu_0}{\nu_i}\right)^4\right)^{-1} \tag{10}$$

is chosen as switching function, where ν_0 is the user defined rotor cutoff value, typically set between 20 and 100 cm^{-1}. The modified vibrational partition function thus corresponds to

the partition function of a harmonic oscillator for high-frequency modes and to that of a hindered rotor for low-frequency modes.

1.2 Cluster Generation

The structures for the neat acetonitrile and (R)-butan-2-ol clusters were taken from previous studies[12,13] and reoptimized at the respective levels of theory. The mixed acetonitrile/(R)-butan-2-ol clusters were created in a systematic cluster generation based on a genetic structure optimization at a classical force field level. For this purpose, we interfaced the OGOLEM[14,15] framework with the AMBER 2016 molecular dynamics package[16] and employed the generalized Amber force field (GAFF).[17] From all generated clusters, the three lowest energy conformers were included in the cluster set. The maximum cluster size corresponds to six monomers for the neat as well as for the mixed clusters. Throughout this work, the clusters will be labeled as aXbY-Z, with X being the number of acetonitrile (a) monomers and Y being the number of (R)-butan-2-ol (b) monomers that are contained in the respective cluster. Z numbers clusters that have the same composition.

1.3 Quantum Chemical Calculations

All quantum chemical calculations were performed using the Turbomole 7.5 software package.[18–21] Four different levels of theory were employed for the geometry optimizations and frequency calculations: BP86[22,23]/def2-SVP,[24] BP86/def2-TZVP,[24] B3LYP[22,23]/def2-SVP and B3LYP/def2-TZVP. London dispersion interactions were modeled by the D3 dispersion correction employing Becke–Johnson damping[25,26] and the geometrical counterpoise correction[27] was used in order to correct for the inter- as well as intramolecular basis set superposition error. The convergence criteria for the self-consistent field energy and the maximum norm of the Cartesian gradient were set to 10^{-8} a.u. and 10^{-4} a.u., respectively. All clusters were verified as minimum structures by having no negative eigenvalues of the Hessian. The IR and VCD spectra were broadened with Gaussian and Lorentzian band shapes, respec-

tively, using a full width at half-maximum of $8\,\mathrm{cm}^{-1}$. To achieve a better agreement with the experimental references, the calculated spectra have been scaled according to the scaling factors reported in Ref.[28]

1.4 Cluster Weighting Calculations

The QCE and bQCE equilibrium populations or so called cluster weights (CWs) were calculated with our publicly available software package PEACEMAKER 2.8.[2,4–6] All calculations were performed within a temperature range of 200–500 K using increments of 1 K and a fixed pressure of 101.325 kPa. The cluster volumes were defined based on van der Waals radii from Bondi's compilation[29] and the mRRHO rotor cutoff value was set to $50\,\mathrm{cm}^{-1}$, which is a robust choice for the calculation of QCE populations.[30] In this work, we consider a linear temperature dependence of b_{xv} (see Equation (6)),[9] which means that the three empirical QCE parameters a_{mf}, β_{xv} and b^0_{xv} are optimized such that the deviation from the given reference data is minimized. For this purpose, the PEACEMAKER 2.8 code is interfaced with the Differential Evolution algorithm[31] from the SciPy library[32] for PYTHON 3.4. The corresponding script can be provided on request. As experimental reference data, the density at 293.15 K, the boiling temperature, and an isobar of the molar volume were employed. The composition of the investigated mixtures is given by the mole fraction $\mathrm{x_b}$ of (R)-butan-2-ol which has been scanned from $\mathrm{x_b} = 0.0$ to $\mathrm{x_b} = 1.0$ in steps of 0.1. The exact values of the reference data and optimized QCE parameters are provided in the Supporting Information. For the weighting of the individual cluster spectra, the cluster weights at 298.15 K have been employed.

1.5 Experimental Setup

Fourier-Transform infrared (FTIR) spectra were recorded at room temperature on a Nicolet 5700 FTIR spectrometer (Thermo Electron Corp.) in transmission mode. Each spectrum is the average of 128 scans measured from 1000 to $7400\,\mathrm{cm}^{-1}$ at a frequency resolution of

$0.5\,\mathrm{cm}^{-1}$. Measurements were repeated three times with freshly prepared samples to ensure reproducibility. The sample cells had a thickness of ≈50 µm and were equipped with CaF_2 windows.

Samples at different molar fractions were prepared from neat solutions of (*R*)-butan-2-ol (98 %, Thermo Scientific Chemicals, $10.9\,\mathrm{mol\,L^{-1}}$) and acetonitrile (≥99.9 %, VWR Chemicals, $19.0\,\mathrm{mol\,L^{-1}}$) which were used without further purification. The concentration of (*R*)-butan-2-ol in mixtures with mole fractions of 0.2, 0.5 and 0.8 corresponds to $3.31\,\mathrm{mol\,L^{-1}}$, $6.94\,\mathrm{mol\,L^{-1}}$ and $9.56\,\mathrm{mol\,L^{-1}}$, respectively.

2 Experimental Reference Data for QCE Calculations

Table S1: Experimental reference data employed in the QCE calculations. x_b corresponds to the mole fraction of (R)-butan-2-ol, $\rho_{293.15}$ is the density at 293.15 K in $g\,cm^{-3}$, T_b the boiling temperature in K and V_T the molar volume at the respective temperature T in L.

x_b	$\rho_{293.15}$	T_b	$V_{293.15}$	$V_{298.15}$	$V_{303.15}$	$V_{308.15}$
0.0	0.7800	355.15	0.05260	0.05300	0.05340	0.05380
0.1	0.7826	356.85	0.05655	0.05695	0.05736	0.05778
0.2	0.7852	358.55	0.06050	0.06090	0.06132	0.06176
0.3	0.7878	360.25	0.06445	0.06485	0.06528	0.06574
0.4	0.7904	361.95	0.06840	0.06880	0.06924	0.06972
0.5	0.7930	363.65	0.07235	0.07275	0.07320	0.07370
0.6	0.7956	365.35	0.07630	0.07670	0.07716	0.07768
0.7	0.7982	367.05	0.08025	0.08065	0.08112	0.08166
0.8	0.8008	368.75	0.08420	0.08460	0.08508	0.08564
0.9	0.8034	370.45	0.08815	0.08855	0.08904	0.08962
1.0	0.8060	372.15	0.09210	0.09250	0.09300	0.09360

3 QCE Parameters

Table S2: Resulting QCE parameters a_{mf} in $J\,m^3\,mol^{-2}$, b^0_{xv} and b_{xv} (both dimensionless) of different optimizations using clusters that were calculated at the BP86/def2-SVP and BP86/def2-TZVP level of theory. x_b corresponds to the mole fraction of (R)-butan-2-ol.

	BP86/def2-SVP			BP86/def2-TZVP		
x_b	a_{mf}	b^0_{xv}	b_{xv}	a_{mf}	b^0_{xv}	b_{xv}
0.0	1.158	0.762	$1.063 \cdot 10^{-3}$	1.116	0.740	$1.158 \cdot 10^{-3}$
0.1	1.266	0.756	$0.953 \cdot 10^{-3}$	1.227	0.733	$1.048 \cdot 10^{-3}$
0.2	1.376	0.745	$0.884 \cdot 10^{-3}$	1.330	0.726	$0.967 \cdot 10^{-3}$
0.3	1.486	0.732	$0.843 \cdot 10^{-3}$	1.430	0.716	$0.913 \cdot 10^{-3}$
0.4	1.594	0.723	$0.802 \cdot 10^{-3}$	1.525	0.709	$0.860 \cdot 10^{-3}$
0.5	1.701	0.713	$0.777 \cdot 10^{-3}$	1.619	0.701	$0.825 \cdot 10^{-3}$
0.6	1.808	0.701	$0.765 \cdot 10^{-3}$	1.709	0.692	$0.802 \cdot 10^{-3}$
0.7	1.913	0.692	$0.752 \cdot 10^{-3}$	1.797	0.684	$0.783 \cdot 10^{-3}$
0.8	2.016	0.682	$0.746 \cdot 10^{-3}$	1.881	0.675	$0.772 \cdot 10^{-3}$
0.9	2.119	0.670	$0.754 \cdot 10^{-3}$	1.960	0.664	$0.777 \cdot 10^{-3}$
1.0	2.224	0.653	$0.788 \cdot 10^{-3}$	2.036	0.647	$0.811 \cdot 10^{-3}$

Table S3: Resulting QCE parameters a_{mf} in $J\,m^3\,mol^{-2}$, b^0_{xv} and b_{xv} (both dimensionless) of different optimizations using clusters that were calculated at the B3LYP/def2-SVP and B3LYP/def2-TZVP level of theory. x_b corresponds to the mole fraction of (R)-butan-2-ol.

	B3LYP/def2-SVP			B3LYP/def2-TZVP		
x_b	a_{mf}	b^0_{xv}	b_{xv}	a_{mf}	b^0_{xv}	b_{xv}
0.0	1.104	0.735	$1.177 \cdot 10^{-3}$	1.062	0.723	$1.221 \cdot 10^{-3}$
0.1	1.216	0.730	$1.061 \cdot 10^{-3}$	1.178	0.720	$1.100 \cdot 10^{-3}$
0.2	1.330	0.723	$0.979 \cdot 10^{-3}$	1.290	0.713	$1.016 \cdot 10^{-3}$
0.3	1.443	0.713	$0.925 \cdot 10^{-3}$	1.399	0.704	$0.957 \cdot 10^{-3}$
0.4	1.554	0.707	$0.872 \cdot 10^{-3}$	1.506	0.699	$0.900 \cdot 10^{-3}$
0.5	1.665	0.699	$0.837 \cdot 10^{-3}$	1.611	0.693	$0.861 \cdot 10^{-3}$
0.6	1.775	0.690	$0.813 \cdot 10^{-3}$	1.715	0.685	$0.833 \cdot 10^{-3}$
0.7	1.884	0.682	$0.792 \cdot 10^{-3}$	1.816	0.678	$0.807 \cdot 10^{-3}$
0.8	1.989	0.675	$0.777 \cdot 10^{-3}$	1.913	0.672	$0.789 \cdot 10^{-3}$
0.9	2.093	0.665	$0.774 \cdot 10^{-3}$	2.006	0.663	$0.784 \cdot 10^{-3}$
1.0	2.194	0.651	$0.797 \cdot 10^{-3}$	2.093	0.648	$0.805 \cdot 10^{-3}$

4 Cluster Weighted Spectra of the Neat Substances

4.1 Infrared

Here we want to examine the neat liquid states of both solvents. Intermolecular interactions are known to have a huge influence on the vibrational modes of a molecule, causing observable differences between the gas phase and liquid phase vibrational spectra.[13,28,33] In the case of liquid acetonitrile, dipole–dipole interactions of the nitrile groups are known to affect the C≡N stretching vibration, greatly enhancing its IR intensity in the liquid phase as compared to the gas phase. The vibrational frequencies of acetonitrile are, however, hardly changed under aggregation.[33]

Figure S1 shows the calculated IR spectra of acetonitrile based on the CWs that were obtained from the PEACEMAKER calculation with $x_b = 0.0$. The calculated spectra show an overall good agreement with the experimentally measured IR spectrum of liquid acetonitrile. Almost all peak positions are modeled correctly and the deviations from the experimentally observed peak locations are mostly less than $10\,\mathrm{cm}^{-1}$. Two exceptions are the symmetric C≡N and the symmetric/asymmetric C−H stretching vibrations which are experimentally observed at around $2252\,\mathrm{cm}^{-1}$ and $2942/3001\,\mathrm{cm}^{-1}$, respectively.[34] These modes are shifted to higher wavenumbers, the symmetric C−H stretching by 25–45 cm^{-1}, and the symmetric C≡N and asymmetric C−H stretching by 40–80 cm^{-1}, depending on the level of theory.

Despite the good agreement of the frequencies, some discrepancies are observed for the intensity ratios, e.g., the intensities in the C−H stretching region around $3000\,\mathrm{cm}^{-1}$ are consistently overestimated at all levels of theory. Accurate and quantitative predictions of vibrational intensities usually require a sophisticated treatment of the electron correlation and large basis sets.[35] However, as we are aiming for a low cost approach that can model the main features of liquid phase spectra, we focus more on using computationally fast quantum chemical methods and consider intensity ratios only qualitatively. The main feature of the acetonitrile liquid phase spectrum, i.e., the high intensity of the C≡N stretching mode at

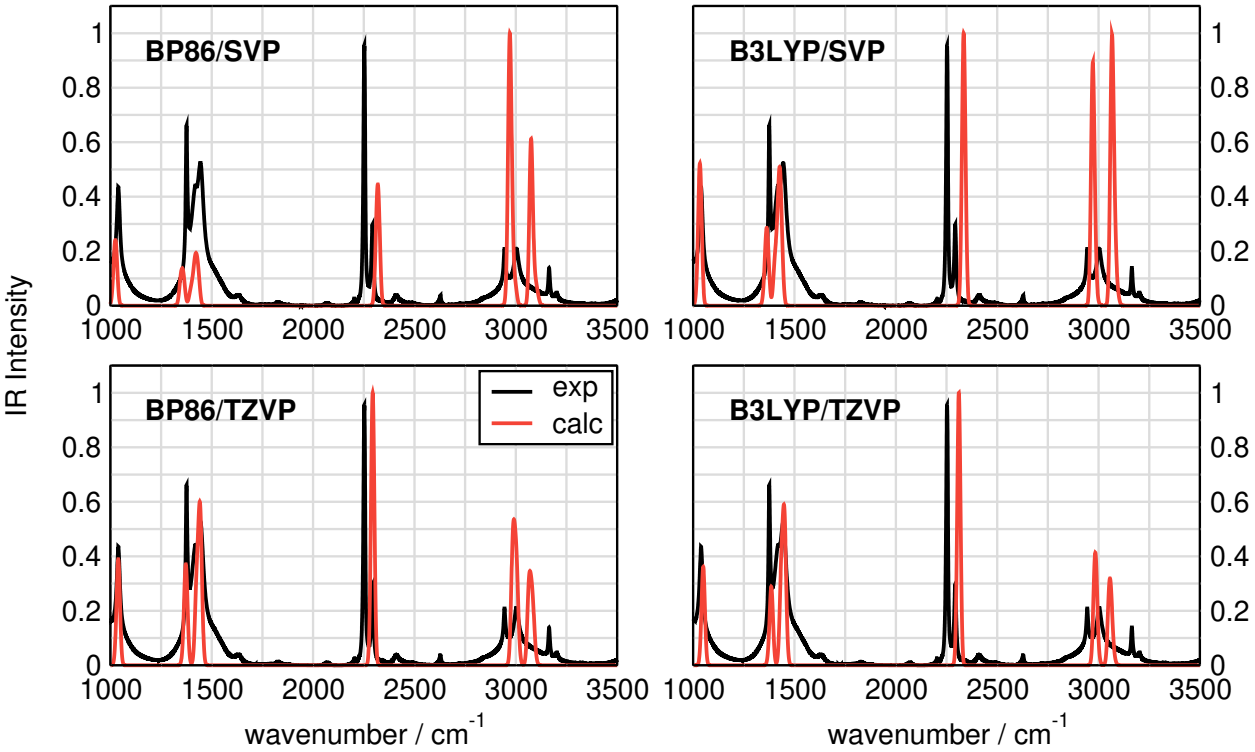

Figure S1: Calculated IR spectra of acetonitrile obtained from cluster weighting compared to the experimental IR spectrum of liquid acetonitrile.

2252 cm^{-1}, is nicely captured by the BP86/TZVP and B3LYP/TZVP spectra. This high intensity can not be modeled by using an isolated acetonitrile monomer only (see Figure S4). The two levels using the smaller SVP basis set produce a worse agreement in this regard, showing that an increase of the basis set indeed improves the intensity ratios of the calculated spectra. Additionally, the intensity of the symmetric CH_3 deformation at 1374 cm^{-1}[34] is increased in the cluster weighted spectrum as compared to the monomer spectrum (see Figure S4), further improving the overlap with the experiment significantly.

To quantify the quality of the cluster weighting approach, Table S4 summarizes the overlaps σ between the experimental liquid phase and the calculated CW spectra. The overlaps are calculated using the SimVCD measure and can range from 0 to +1 in the case of IR and from −1 to +1 in the case of VCD spectra.[36] The best agreement with the experiment is observed for BP86/TZVP with an overlap of 0.614, followed by an overlap of 0.533 for the B3LYP/TZVP spectrum. As already concluded from the visual inspection, the

Table S4: Overlap σ between the experimental bulk phase and calculated CW spectra of neat acetonitrile (IR_a) and (R)-butan-2-ol (IR_b and VCD_b). The values in parentheses correspond to the overlaps between the experimental bulk phase spectra and calculated monomer spectra. The overlap is calculated with the SimIR/VCD tool[36] and can range from 0 to +1 for IR and from −1 to +1 for VCD.

	BP86/SVP	BP86/TZVP	B3LYP/SVP	B3LYP/TZVP
IR_a	0.429 (0.279)	0.614 (0.307)	0.519 (0.224)	0.533 (0.274)
IR_b	0.570 (0.400)	0.653 (0.377)	0.571 (0.385)	0.584 (0.343)
VCD_b	0.166 (0.184)	0.240 (0.129)	0.296 (0.181)	0.290 (0.163)

two levels of theory using the small SVP basis set yield a poorer overlap with the experiment, which is mostly caused by the inaccurate intensity ratios. Table S4 additionally summarizes the overlaps between the experimental bulk phase spectra and calculated monomer spectra (see Figure S4). Based on these overlaps, it becomes clear that using only the acetonitrile monomer yields a much poorer overlap with the experimental bulk phase spectrum, justifying the application of our cluster weighting approach for the calculation of liquid phase spectra.

(R)-butan-2-ol molecules are known to aggregate in the liquid phase, mainly by hydrogen bonds. These hydrogen bonds usually induce large frequency shifts and intensity perturbations in liquid phase spectra compared to the gas phase. The most pronounced frequency shifts are observed for the C−O stretching and C−O−H bending modes which are shifted from 1076 cm^{-1} and 1241 cm^{-1} to the region of H−C−H bending modes around 1450 cm^{-1}.[37,38] We have already discussed the functional and basis set dependence of cluster weighted IR and VCD spectra of (R)-butan-2-ol in an earlier study.[28] Although we are using a different cluster set herein, we observe the same trends and will therefore only briefly discuss the spectra of neat (R)-butan-2-ol in the following. For a more detailed discussion the reader is referred to Refs.[13,28]

Figure S2 shows the calculated IR spectra of (R)-butan-2-ol based on the CWs that were obtained from the PEACEMAKER calculation with $x_b = 1.0$. The spectra show a good agreement with the experimental spectrum of liquid (R)-butan-2-ol and the peak positions and intensities below 1200 cm^{-1} are reproduced almost perfectly, especially for BP86/TZVP

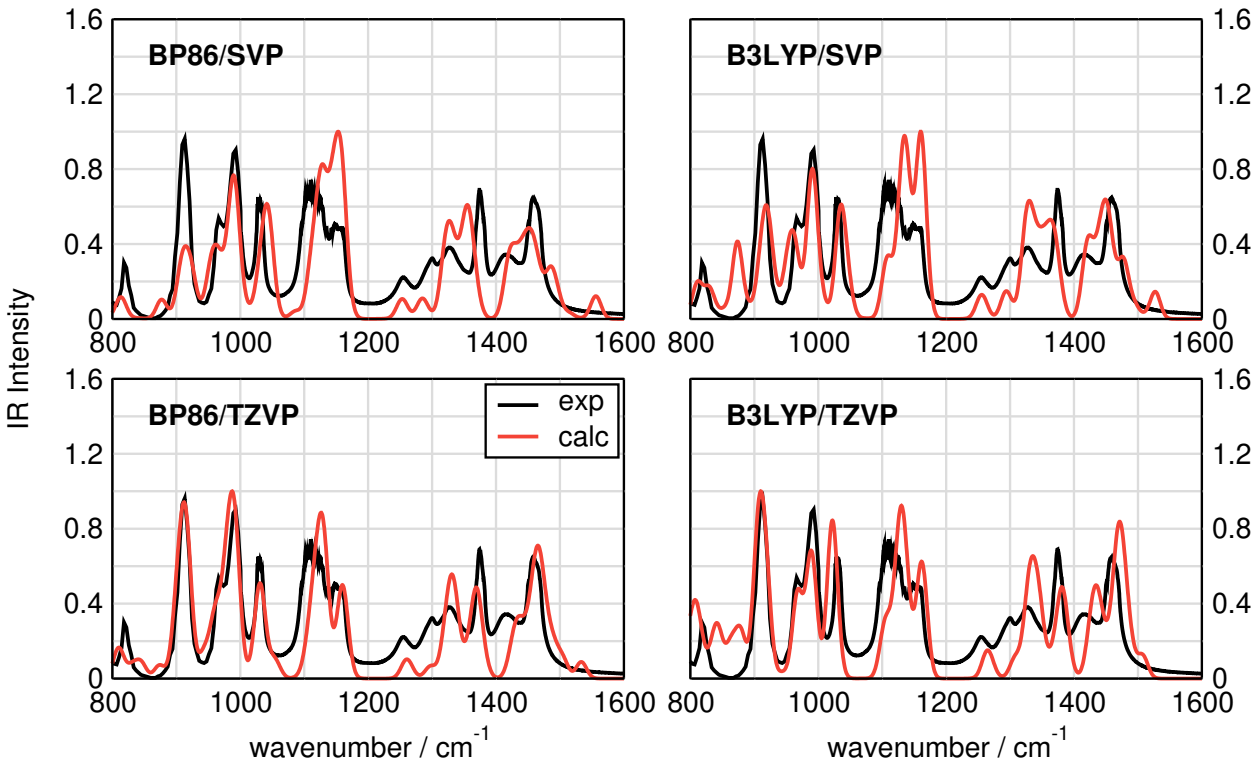

Figure S2: Calculated IR spectra of (R)-butan-2-ol obtained from cluster weighting compared to the experimental IR spectrum of liquid (R)-butan-2-ol. The experimental spectrum below $1000\,\mathrm{cm}^{-1}$ is reproduced from Ref.[37]

and B3LYP/TZVP. For the broader band between 1200 and $1500\,\mathrm{cm}^{-1}$ we observe some discrepancies, mainly underestimated intensities for the H−C−H bending modes between 1200 and $1300\,\mathrm{cm}^{-1}$ and around $1400\,\mathrm{cm}^{-1}$. Performing a normal mode analysis of the (R)-butan-2-ol monomers reveals, that the C−O−H bending modes are located between 1200 and $1300\,\mathrm{cm}^{-1}$, see Figure S5 for the monomer IR spectra of (R)-butan-2-ol. This agrees well with experimentally recorded IR spectra of a 0.029 M (R)-butan-2-ol solution in carbon disulfide,[37] which can be seen as a gas phase reference. However, a normal mode analysis of the clusters that contribute to the IR spectra shown in Figure S2 reveals that their C−O−H bending modes are shifted to $1450\,\mathrm{cm}^{-1}$, just as it is observed in the experimental spectrum of the liquid phase. We observed earlier that the sole application of an implicit solvation model to the (R)-butan-2-ol monomers is not sufficient to model this hydrogen bond induced frequency shift,[13] showing that it is necessary to use clusters here. This is further exemplified

by the overlaps summarized in Table S4, which show that the monomer spectra have a worse overlap with the liquid phase experiment than the cluster weighted spectra. Again, the best agreement with the experiment is observed for BP86/TZVP with an overlap of $\sigma = 0.653$, the remaining levels of theory perform similarly well and yield overlaps between 0.570 and 0.584.

4.2 Vibrational Circular Dichroism

Figure S3 depicts the cluster weighted VCD spectra for (R)-butan-2-ol which show a satisfactory agreement with the experiment between 1120 and 1500 cm^{-1} and the intense negative peak around 1150 cm^{-1} is nicely captured by all levels of theory. Compared to the calculated monomer VCD spectra (see Figure S6), i.e., the gas phase reference, the most important change in the cluster weighted spectra is the vanishing positive peak around 1250 cm^{-1}. In the gas phase, this peak corresponds to the C−O−H bending mode and its shift to the region of H−C−H bending modes around 1450 cm^{-1} leads to the disappearance of this peak in the liquid phase. This main characteristics of the experimental liquid phase VCD spectrum is nicely reproduced by the cluster weighted spectra. Again, we observed earlier that the sole application of a continuum solvation model is not sufficient to model this feature of the liquid phase VCD spectrum.[13] Below 1150 cm^{-1} the agreement with the experiment is worse. Especially the intense positive peak at 1110 cm^{-1}, corresponding to C−O stretching and C−C−H bending motions, is barely reproduced by any level of theory but rather redshifted by 60–80 cm^{-1}.

In the case of VCD, overlaps of 0.2 and greater usually allow for a safe ($> 90\%$) determination of the absolute configuration. The overlaps of the calculated monomer VCD spectra (see Figure S6) with the liquid phase experiment are, however, consistently smaller than 0.2 (see Table S4). The cluster weighted VCD spectra improve the overlap with the experiment with the exception of BP86/SVP. In the case of BP86/SVP, the poor overlap is most likely caused by the high intensity of the positive peak around 1050 cm^{-1}. Besides that,

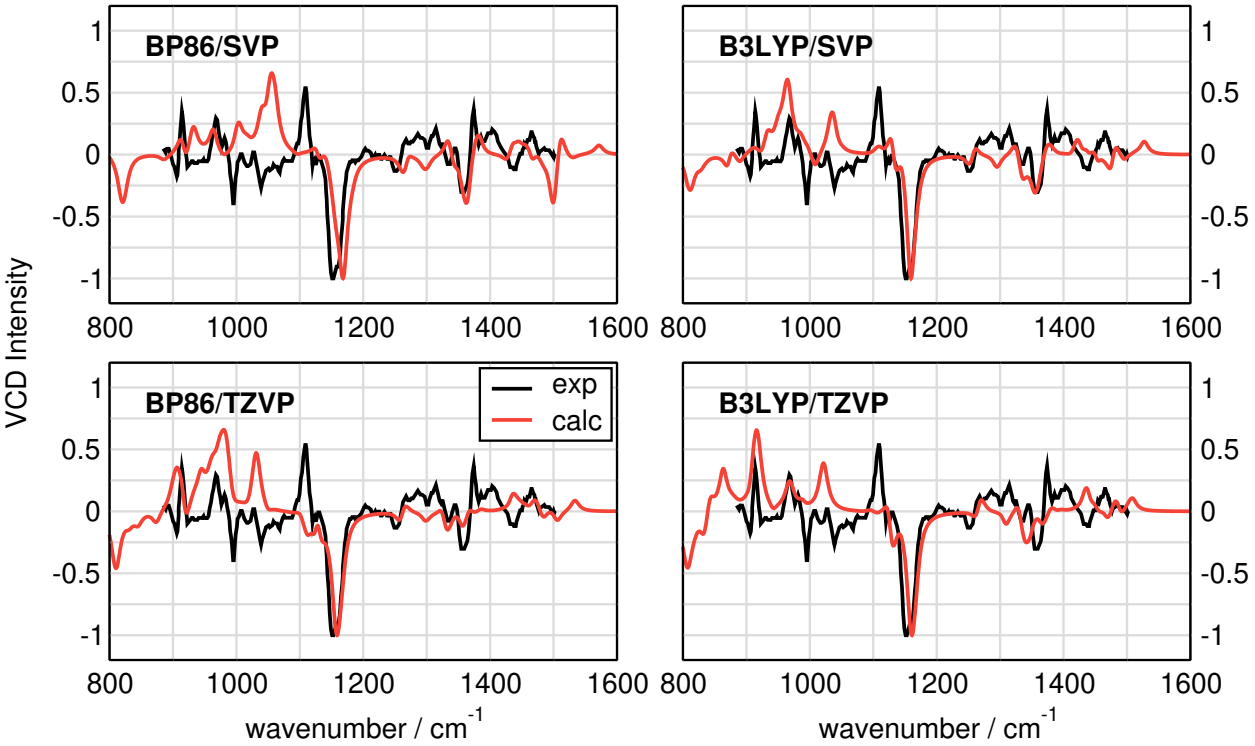

Figure S3: Calculated VCD spectra of (R)-butan-2-ol obtained from cluster weighting compared to the experimental VCD spectrum[37] of liquid (R)-butan-2-ol.

the overlaps achieved by the other levels of theory are greater than 0.2, which allows for a certain assignment of the absolute configuration based on the liquid phase VCD spectrum.

4.3 Monomer Spectra

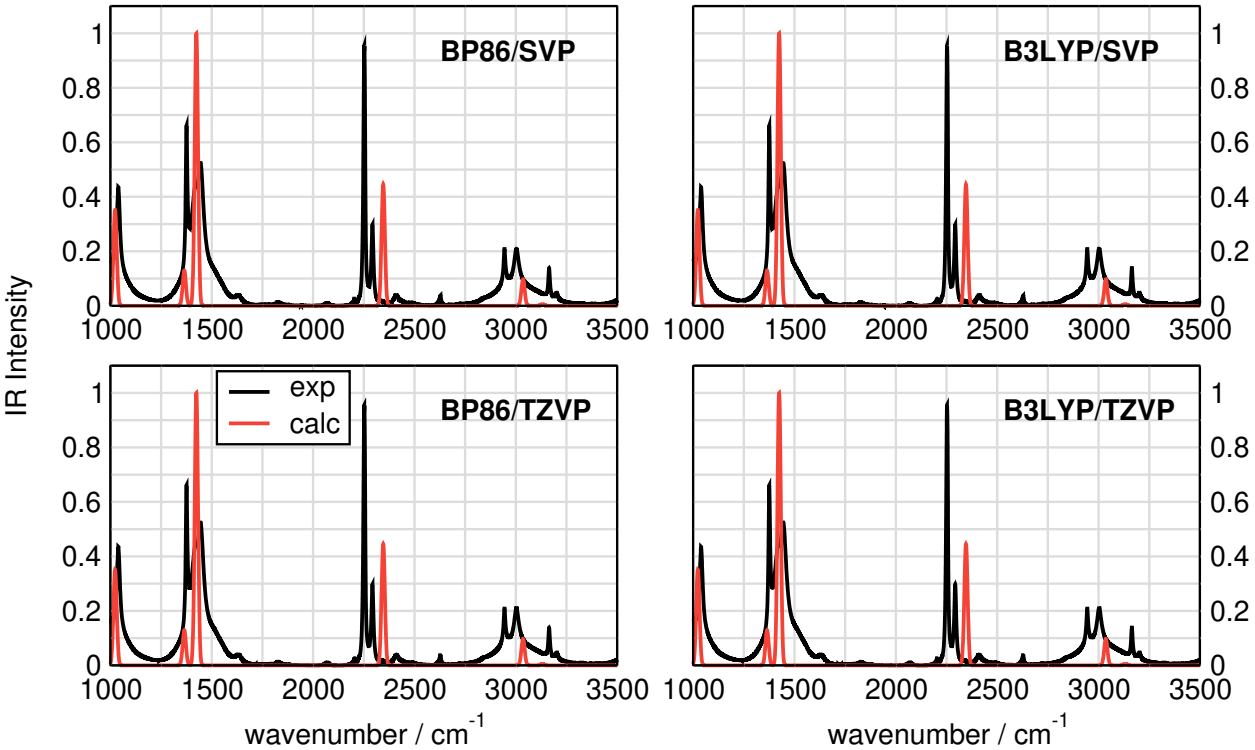

Figure S4: IR spectrum of the acetonitrile monomer at different levels of theory compared to the experimental IR spectrum of liquid acetonitrile.

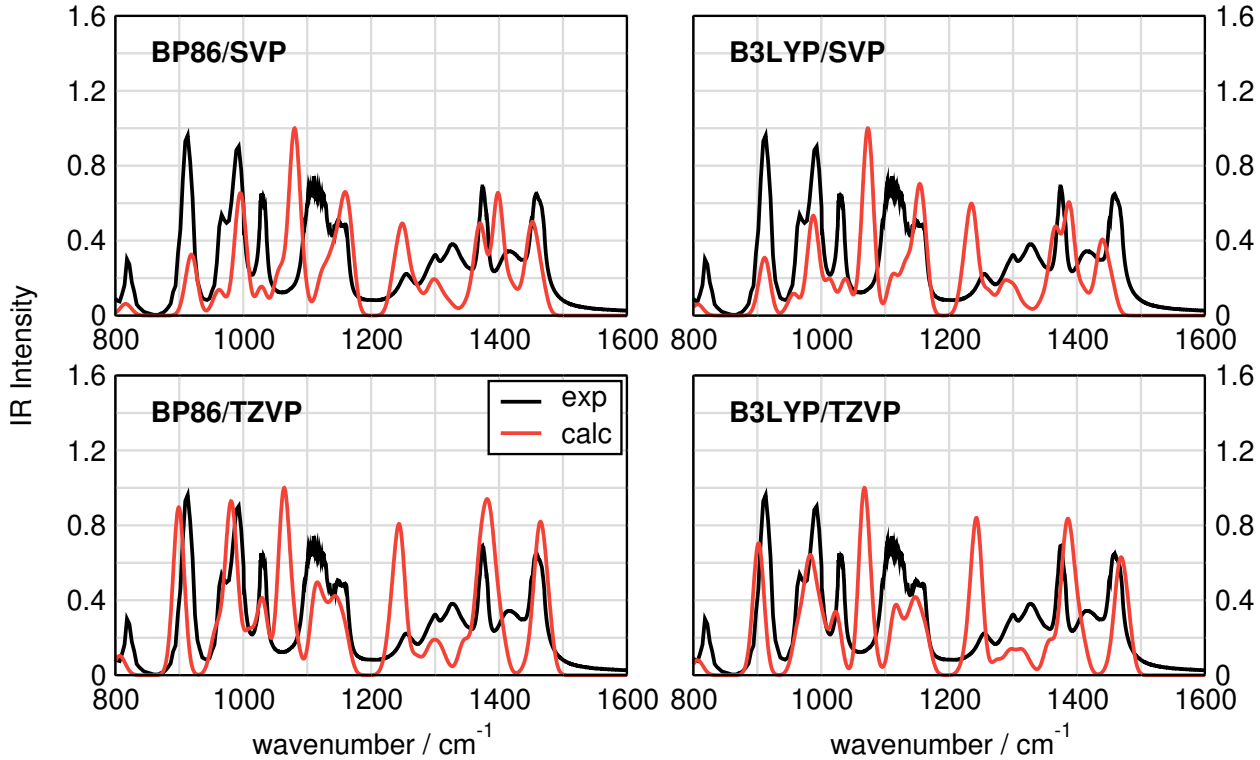

Figure S5: Cluster weighted IR spectrum of the (R)-butan-2-ol monomers at different levels of theory compared to the experimental IR spectrum of liquid (R)-butan-2-ol. The CWs were obtained from a PEACEMAKER calculation with $x_b = 1.0$ employing only the monomer conformers in the cluster set.

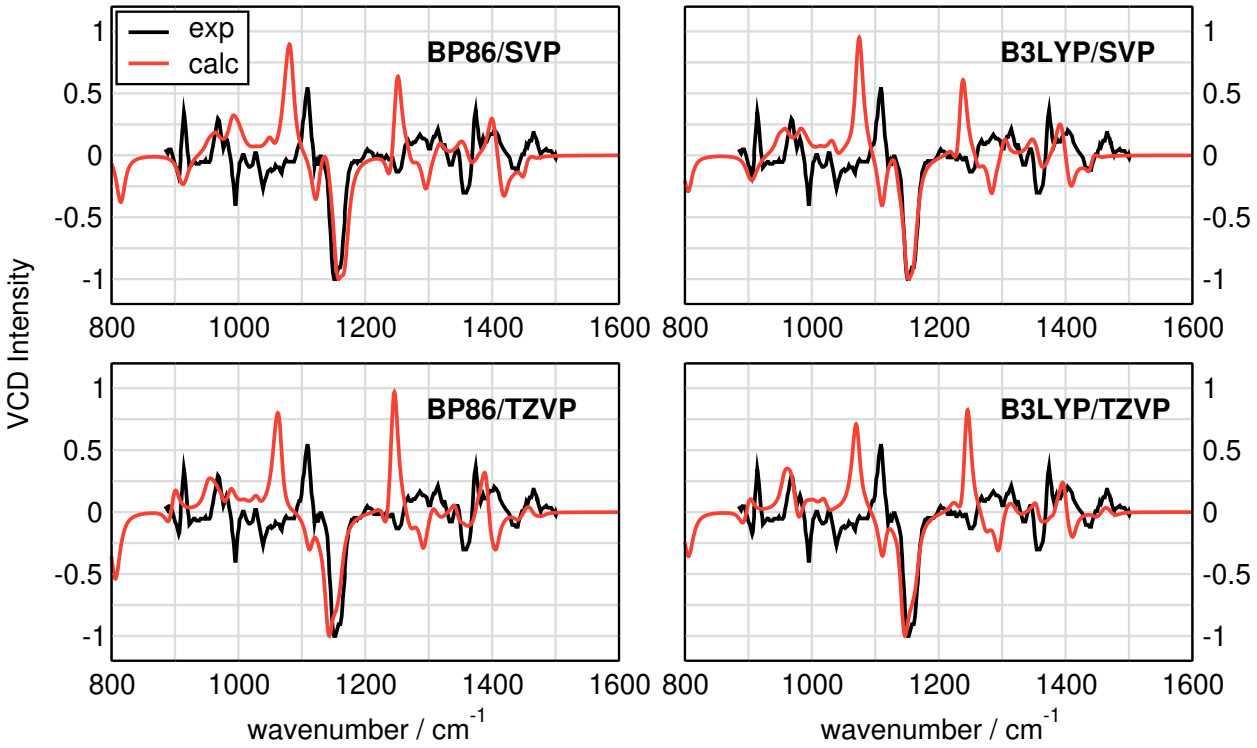

Figure S6: Cluster weighted VCD spectrum of the (R)-butan-2-ol monomers at different levels of theory compared to the experimental VCD spectrum of liquid (R)-butan-2-ol.[37] The CWs were obtained from a PEACEMAKER calculation with $x_b = 1.0$ employing only the monomer conformers in the cluster set.

5 Cluster Weighted Spectra of Mixtures

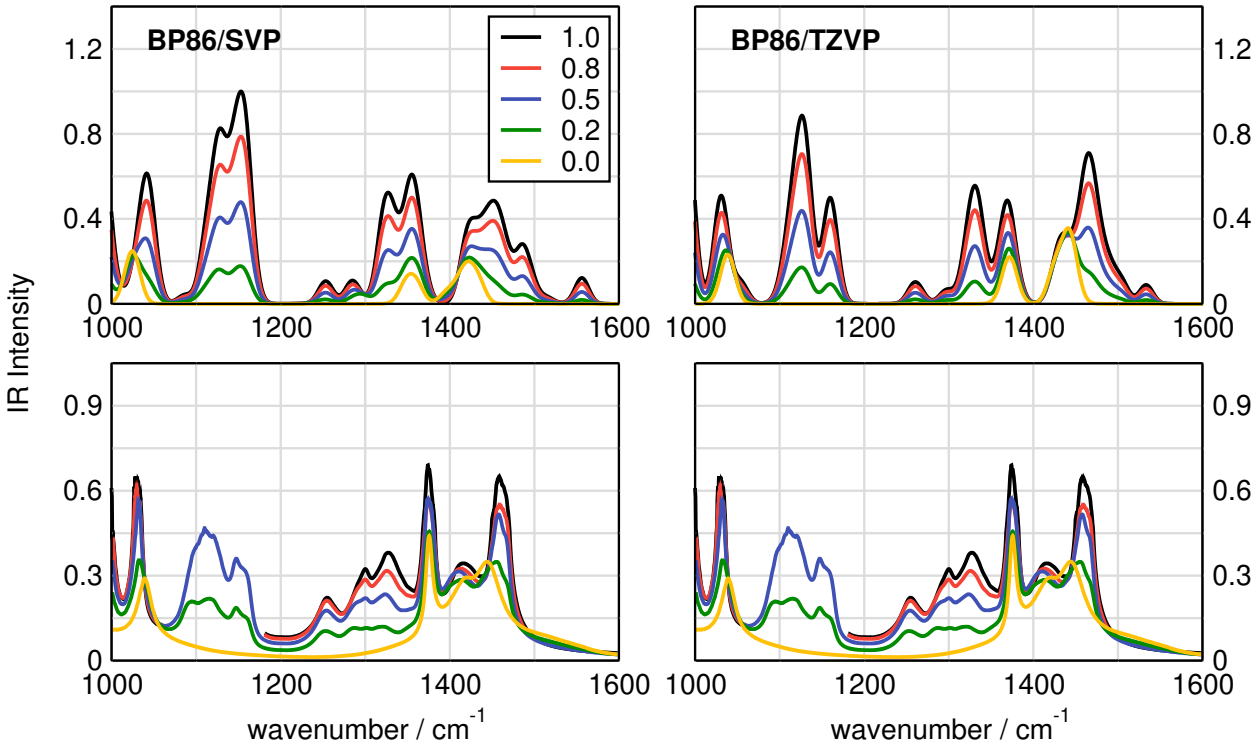

Figure S7: Top: Cluster weighted IR spectra of acetonitrile/(*R*)-butan-2-ol mixtures with varying composition obtained at the BP86/SVP and BP86/TZVP levels of theory. The composition is given by the mole fraction x_b of (*R*)-butan-2-ol. Bottom: Experimental IR spectra recorded in transmission mode. Note that for 1.0 and 0.8 the experimental data between 1060–1180 cm^{-1} had to be excluded due to an oversaturation of the detector..

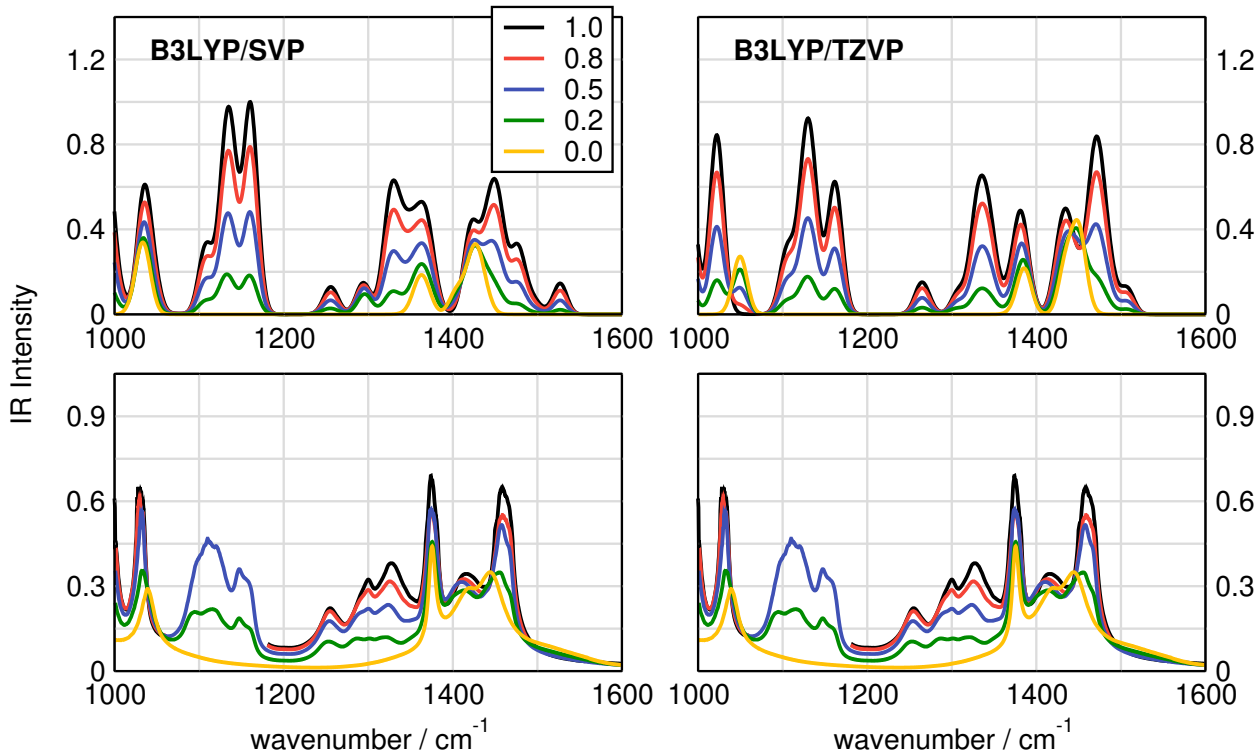

Figure S8: Top: Cluster weighted IR spectra of acetonitrile/(*R*)-butan-2-ol mixtures with varying composition obtained at the B3LYP/SVP and B3LYP/TZVP levels of theory. The composition is given by the mole fraction x_b of (*R*)-butan-2-ol. Bottom: Experimental IR spectra recorded in transmission mode. Note that for 1.0 and 0.8 the experimental data between 1060–1180 cm^{-1} had to be excluded due to an oversaturation of the detector.

Table S5: Averaged relative peak intensities for the VCD spectra obtained at different mole fractions with respect to the VCD spectra obtained at $x_b = 1.0$.

x_b	BP86/SVP	BP86/TZVP	B3LYP/SVP	B3LYP/TZVP
0.2	0.22	0.20	0.21	0.22
0.5	0.50	0.48	0.45	0.51
0.8	0.79	0.79	0.77	0.81
1.0	1.00	1.00	1.00	1.00

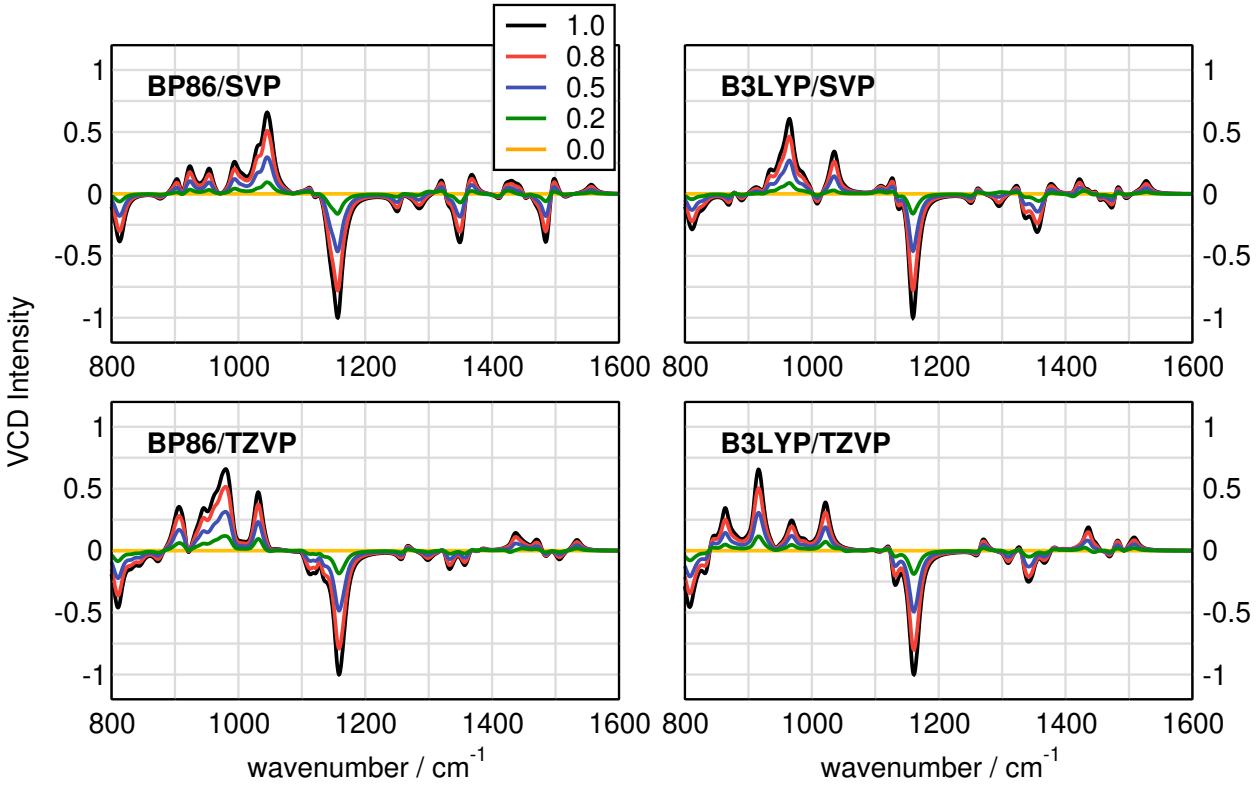

Figure S9: Cluster weighted VCD spectra of acetonitrile/(R)-butan-2-ol mixtures with varying composition obtained at different levels of theory. The composition is given by the mole fraction x_b of (R)-butan-2-ol.

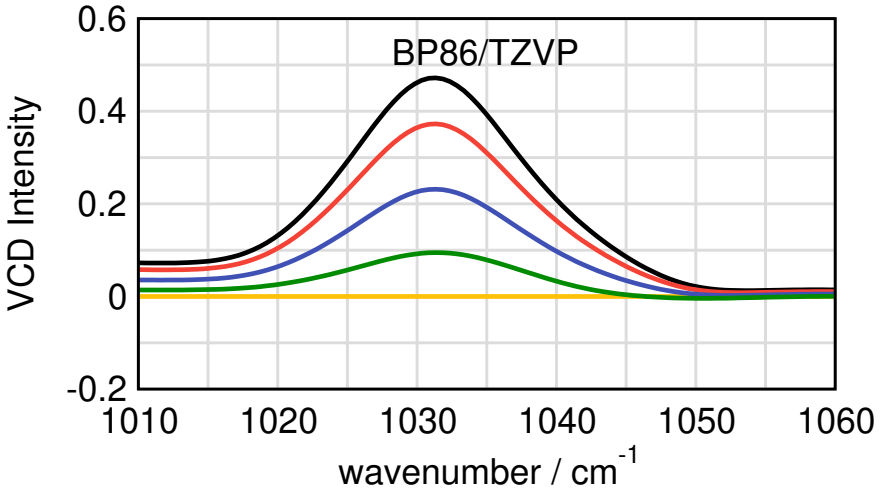

Figure S10: Cluster weighted VCD spectra of acetonitrile/(R)-butan-2-ol mixtures with varying compositions between 1010–1060 cm^{-1}. The composition is given by the mole fraction x_b of (R)-butan-2-ol.

6 Cluster Populations

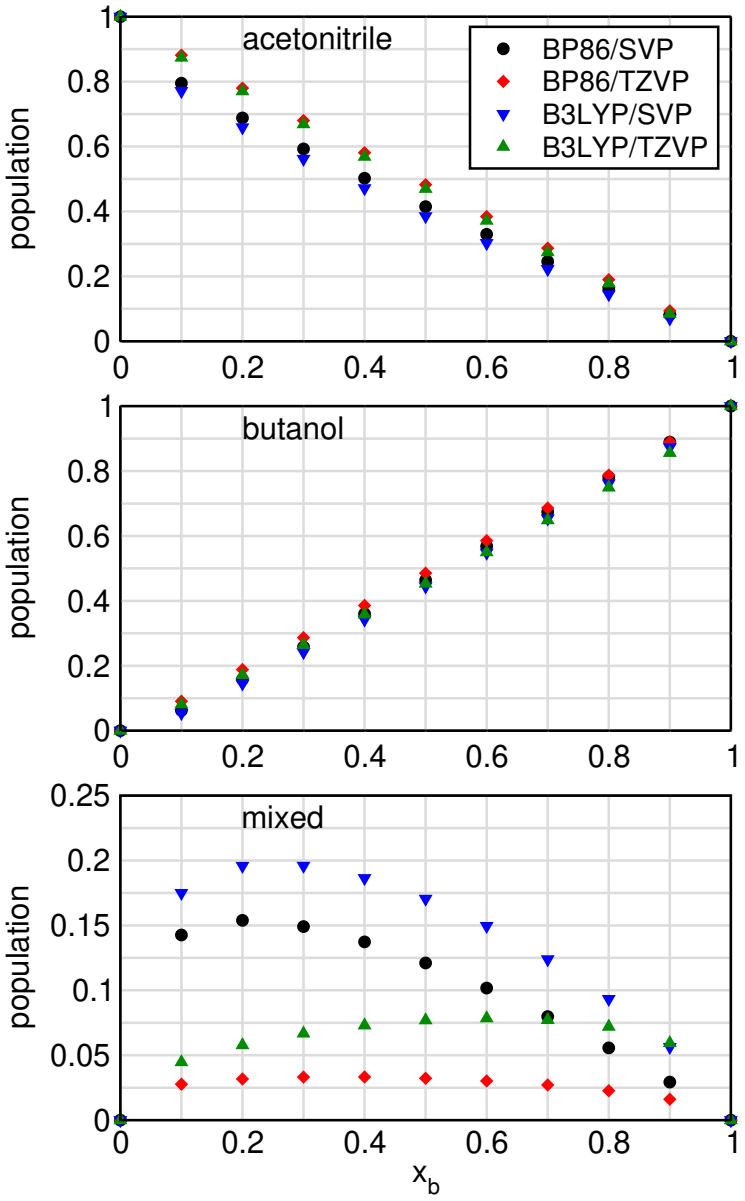

Figure S11: Summed up populations at 298.15 K of pure and mixed clusters of the binary acetonitrile/butanol mixture at different mole fractions. Each panel corresponds to a different species of clusters: neat acetonitrile, neat butanol and mixed clusters.

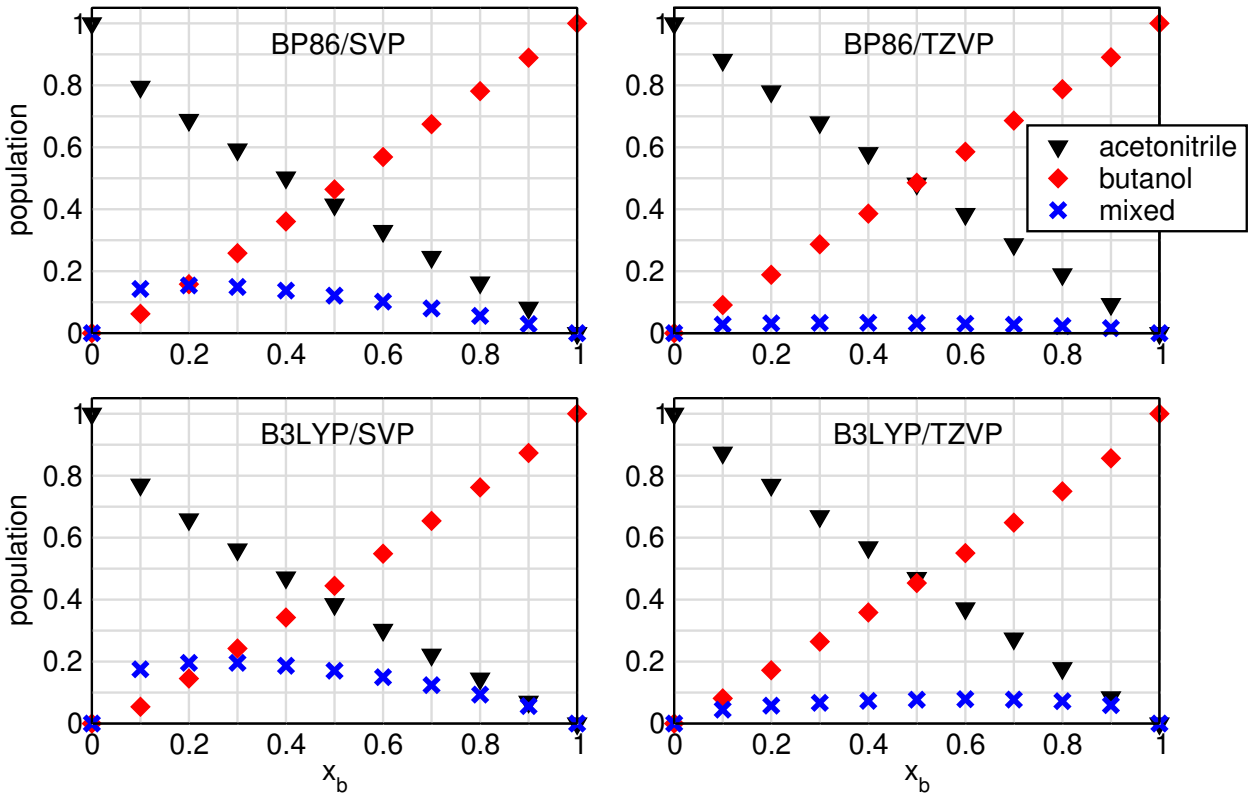

Figure S12: Summed up populations at 298.15 K of neat and mixed clusters of the binary acetonitrile/butanol mixture at different mole fractions. Each panel corresponds to a different level of theory.

7 Cluster Energies

Table S6: Energies of the acetonitrile clusters at the BP86/def2-SVP level of theory. E_{elec} is the electronic energy, E_{gCP} is the geometrical counterpoise correction and E_{tot} is the sum of both, all three given in hartree. ΔE is the relative energy and $\Delta E/n$ is the relative energy divided by the number of molecules n contained in a cluster, both given in $\mathrm{kJ\,mol^{-1}}$.

	BP86/def2-SVP				
cluster	E_{elec}	E_{gCP}	E_{tot}	ΔE	$\Delta E/n$
a1-1	-132.663218	0.015364	-132.647853	0.0	0.0
a2-1	-265.338257	0.033039	-265.305218	-24.97	-12.49
a3-1	-398.014491	0.049848	-397.964643	-55.35	-18.45
a4-1	-530.694974	0.070546	-530.624428	-86.68	-21.67
a4-2	-530.694769	0.070482	-530.624287	-86.31	-21.58
a5-1	-663.370539	0.087610	-663.282929	-114.63	-22.93
a5-2	-663.369709	0.087809	-663.281820	-111.72	-22.34
a5-3	-663.369010	0.088703	-663.280307	-107.75	-21.55
a6-1	-796.050975	0.106033	-795.944941	-151.81	-25.30
a6-2	-796.049832	0.107189	-795.942643	-145.78	-24.30
a6-3	-796.048769	0.107599	-795.941170	-141.91	-23.65

Table S7: Energies of the acetonitrile clusters at the BP86/def2-TZVP level of theory. E_{elec} is the electronic energy, E_{gCP} is the geometrical counterpoise correction and E_{tot} is the sum of both, all three given in hartree. ΔE is the relative energy and $\Delta E/n$ is the relative energy divided by the number of molecules n contained in a cluster, both given in $\mathrm{kJ\,mol^{-1}}$.

	BP86/def2-TZVP				
cluster	E_{elec}	E_{gCP}	E_{tot}	ΔE	$\Delta E/n$
a1-1	-132.815718	0.002965	-132.812753	0.00	0.00
a2-1	-265.641226	0.006210	-265.635016	-24.97	-12.48
a3-1	-398.466300	0.009342	-398.456959	-49.10	-16.37
a4-1	-531.297502	0.012998	-531.284504	-87.94	-21.98
a4-2	-531.297265	0.012968	-531.284297	-87.39	-21.85
a5-1	-664.122149	0.016223	-664.105925	-110.70	-22.14
a5-2	-664.121794	0.016196	-664.105598	-109.84	-21.97
a5-3	-664.121775	0.016362	-664.105413	-109.35	-21.87
a6-1	-796.951354	0.019612	-796.931742	-144.99	-24.17
a6-2	-796.952104	0.019762	-796.932342	-146.57	-24.43
a6-3	-796.950138	0.019749	-796.930389	-141.44	-23.57

Table S8: Energies of the acetonitrile clusters at the B3LYP/def2-SVP level of theory. E_{elec} is the electronic energy, E_{gCP} is the geometrical counterpoise correction and E_{tot} is the sum of both, all three given in hartree. ΔE is the relative energy and $\Delta E/n$ is the relative energy divided by the number of molecules n contained in a cluster, both given in $\mathrm{kJ\,mol^{-1}}$.

	B3LYP/def2-SVP				
cluster	E_{elec}	E_{gCP}	E_{tot}	ΔE	$\Delta E/n$
a1-1	-132.578831	0.015545	-132.563286	0.00	0.00
a2-1	-265.170149	0.033284	-265.136865	-27.02	-13.51
a3-1	-397.762199	0.050143	-397.712057	-58.28	-19.43
a4-1	-530.359828	0.070787	-530.289042	-94.25	-23.56
a4-2	-530.359798	0.070768	-530.289030	-94.22	-23.55
a5-1	-662.951232	0.087839	-662.863392	-123.30	-24.66
a5-2	-662.950947	0.088269	-662.862678	-121.42	-24.28
a5-3	-662.950398	0.089155	-662.861243	-117.65	-23.53
a6-1	-795.548107	0.106318	-795.441789	-162.97	-27.16
a6-2	-795.547915	0.108004	-795.439911	-158.04	-26.34
a6-3	-795.546902	0.107924	-795.438979	-155.59	-25.93

Table S9: Energies of the acetonitrile clusters at the B3LYP/def2-TZVP level of theory. E_{elec} is the electronic energy, E_{gCP} is the geometrical counterpoise correction and E_{tot} is the sum of both, all three given in hartree. ΔE is the relative energy and $\Delta E/n$ is the relative energy divided by the number of molecules n contained in a cluster, both given in kJ mol^{-1}.

	B3LYP/def2-TZVP				
cluster	E_{elec}	E_{gCP}	E_{tot}	ΔE	$\Delta E/n$
a1-1	-132.734134	0.003002	-132.731133	0.0	0.0
a2-1	-265.478628	0.006270	-265.472358	-26.50	-13.25
a3-1	-398.222330	0.009421	-398.212909	-51.23	-17.08
a4-1	-530.972958	0.013070	-530.959887	-92.83	-23.21
a4-2	-530.972853	0.013055	-530.959798	-92.59	-23.15
a5-1	-663.716227	0.016311	-663.699916	-116.19	-23.24
a5-2	-663.716285	0.016303	-663.699982	-116.36	-23.27
a5-3	-663.716325	0.016478	-663.699847	-116.01	-23.20
a6-1	-796.464585	0.019719	-796.444866	-152.46	-25.41
a6-2	-796.465850	0.019865	-796.445984	-155.40	-25.90
a6-3	-796.463928	0.019840	-796.444088	-150.42	-25.07

Table S10: Energies of the (R)-butan-2-ol clusters at the BP86/def2-SVP level of theory. E_{elec} is the electronic energy, E_{gCP} is the geometrical counterpoise correction and E_{tot} is the sum of both, all three given in hartree. ΔE is the relative energy and $\Delta E/n$ is the relative energy divided by the number of molecules n contained in a cluster, both given in kJ mol^{-1}.

	BP86/def2-SVP				
cluster	E_{elec}	E_{gCP}	E_{tot}	ΔE	$\Delta E/n$
b1-1	-233.518765	0.052714	-233.466050	0.00	0.00
b1-2	-233.517545	0.052454	-233.465090	2.52	2.52
b1-3	-233.517187	0.052816	-233.464370	4.41	4.41
b1-4	-233.518111	0.052686	-233.465424	1.64	1.64
b1-5	-233.517160	0.052481	-233.464679	3.60	3.60
b1-6	-233.517083	0.052790	-233.464293	4.61	4.61
b1-7	-233.518014	0.052795	-233.465220	2.18	2.18
b1-8	-233.517335	0.052496	-233.464838	3.18	3.18
b1-9	-233.517469	0.052793	-233.464676	3.61	3.61
b2-1	-467.055408	0.112635	-466.942773	-28.02	-14.01
b2-2	-467.054360	0.112420	-466.941940	-25.83	-12.92
b2-3	-467.054312	0.111995	-466.942317	-26.82	-13.41
b2-4	-467.054044	0.112973	-466.941071	-23.55	-11.78
b2-5	-467.053449	0.112038	-466.941411	-24.44	-12.22
b2-6	-467.053666	0.112157	-466.941509	-24.70	-12.35
b2-7	-467.054318	0.113156	-466.941162	-23.79	-11.89
b2-8	-467.052736	0.112153	-466.940583	-22.27	-11.14
b2-9	-467.053628	0.112370	-466.941258	-24.04	-12.02
b3-1	-700.607394	0.179014	-700.428381	-79.37	-26.46
b3-2	-700.605594	0.178435	-700.427159	-76.16	-25.39
b3-3	-700.605494	0.177722	-700.427772	-77.77	-25.92
b3-4	-700.604837	0.176750	-700.428087	-78.60	-26.20
b3-5	-700.605005	0.177089	-700.427916	-78.15	-26.05
b3-6	-700.603956	0.176438	-700.427518	-77.10	-25.70
b3-7	-700.603873	0.176848	-700.427025	-75.81	-25.27
b3-8	-700.603484	0.176836	-700.426648	-74.82	-24.94
b3-9	-700.603628	0.176621	-700.427007	-75.76	-25.25
b3-10	-700.600268	0.175122	-700.425147	-70.88	-23.63
b4-1	-934.164122	0.245563	-933.918560	-142.72	-35.68
b4-2	-934.160199	0.244177	-933.916022	-136.05	-34.01
b4-3	-934.159437	0.243206	-933.916231	-136.60	-34.15
b4-4	-934.160093	0.242506	-933.917587	-140.16	-35.04
b4-5	-934.159027	0.243599	-933.915428	-134.50	-33.62
b4-6	-934.156898	0.241671	-933.915228	-133.97	-33.49
b4-7	-934.159855	0.242933	-933.916923	-138.42	-34.60
b4-8	-934.156401	0.242435	-933.913965	-130.66	-32.66
b4-9	-934.157018	0.243909	-933.913109	-128.41	-32.10
b5-1	-1167.713492	0.308303	-1167.405189	-196.75	-39.35
b5-2	-1167.707720	0.309312	-1167.398408	-178.94	-35.79
b5-3	-1167.696878	0.305499	-1167.391379	-160.49	-32.10
b6-1	-1401.261952	0.372888	-1400.889063	-243.55	-40.59
b6-2	-1401.258479	0.374162	-1400.884317	-231.08	-38.51
b6-3	-1401.250325	0.375478	-1400.874847	-206.22	-34.37
b6-6	-1401.226069	0.362305	-1400.863764	-177.12	-29.52

Table S11: Energies of the (R)-butan-2-ol clusters at the BP86/def2-TZVP level of theory. E_{elec} is the electronic energy, E_{gCP} is the geometrical counterpoise correction and E_{tot} is the sum of both, all three given in hartree. ΔE is the relative energy and $\Delta E/n$ is the relative energy divided by the number of molecules n contained in a cluster, both given in kJ mol^{-1}.

	BP86/def2-TZVP				
cluster	E_{elec}	E_{gCP}	E_{tot}	ΔE	$\Delta E/n$
b1-1	-233.785221	0.010488	-233.774733	0.00	0.00
b1-2	-233.784611	0.010522	-233.774089	1.69	1.69
b1-3	-233.784011	0.010614	-233.773397	3.51	3.51
b1-4	-233.785092	0.010472	-233.774619	0.30	0.30
b1-5	-233.784557	0.010521	-233.774036	1.83	1.83
b1-6	-233.784023	0.010544	-233.773478	3.30	3.30
b1-7	-233.785282	0.010575	-233.774706	0.07	0.07
b1-8	-233.784735	0.010533	-233.774202	1.40	1.40
b1-9	-233.784266	0.010546	-233.773720	2.66	2.66
b2-1	-467.582774	0.022233	-467.560541	-29.08	-14.54
b2-2	-467.581383	0.022191	-467.559192	-25.53	-12.77
b2-3	-467.581554	0.022122	-467.559431	-26.16	-13.08
b2-4	-467.581581	0.022355	-467.559226	-25.62	-12.81
b2-5	-467.581974	0.022157	-467.559817	-27.18	-13.59
b2-6	-467.581606	0.022254	-467.559352	-25.95	-12.98
b2-7	-467.581257	0.022382	-467.558875	-24.70	-12.35
b2-8	-467.580327	0.022173	-467.558154	-22.81	-11.40
b2-9	-467.581207	0.022284	-467.558922	-24.83	-12.41
b3-1	-701.391546	0.035232	-701.356314	-84.31	-28.10
b3-2	-701.390362	0.035077	-701.355285	-81.61	-27.20
b3-3	-701.390782	0.034994	-701.355788	-82.93	-27.64
b3-4	-701.390756	0.034836	-701.355920	-83.28	-27.76
b3-5	-701.390338	0.034862	-701.355477	-82.12	-27.37
b3-6	-701.390258	0.034860	-701.355398	-81.91	-27.30
b3-7	-701.389334	0.034802	-701.354532	-79.64	-26.55
b3-8	-701.388869	0.034751	-701.354118	-78.55	-26.18
b3-9	-701.389106	0.034828	-701.354278	-78.97	-26.32
b3-10	-701.385322	0.034376	-701.350946	-70.22	-23.41
b4-1	-935.205120	0.048244	-935.156876	-152.13	-38.03
b4-2	-935.202929	0.048049	-935.154879	-146.89	-36.72
b4-3	-935.202272	0.047997	-935.154275	-145.30	-36.32
b4-4	-935.202976	0.047622	-935.155355	-148.13	-37.03
b4-5	-935.202453	0.047916	-935.154537	-145.99	-36.50
b4-6	-935.201194	0.047689	-935.153505	-143.28	-35.82
b4-7	-935.202612	0.047843	-935.154769	-146.59	-36.65
b4-8	-935.200608	0.048109	-935.152499	-140.64	-35.16
b4-9	-935.201411	0.047935	-935.153476	-143.20	-35.80
b5-1	-1169.013650	0.060239	-1168.953411	-209.37	-41.87
b5-2	-1169.007271	0.060784	-1168.946488	-191.19	-38.24
b5-3	-1168.998633	0.059938	-1168.938694	-170.73	-34.15
b6-1	-1402.820747	0.073047	-1402.747700	-260.71	-43.45
b6-2	-1402.816409	0.073465	-1402.742944	-248.22	-41.37
b6-3	-1402.811717	0.074105	-1402.737613	-234.23	-39.04
b6-6	-1402.793651	0.071484	-1402.722167	-193.67	-32.28

Table S12: Energies of the (R)-butan-2-ol clusters at the B3LYP/def2-SVP level of theory. E_{elec} is the electronic energy, E_{gCP} is the geometrical counterpoise correction and E_{tot} is the sum of both, all three given in hartree. ΔE is the relative energy and $\Delta E/n$ is the relative energy divided by the number of molecules n contained in a cluster, both given in kJ mol^{-1}.

	B3LYP/def2-SVP				
cluster	E_{elec}	E_{gCP}	E_{tot}	ΔE	$\Delta E/n$
b1-1	-233.364404	0.053340	-233.311064	0.00	0.00
b1-2	-233.363106	0.053095	-233.310011	2.76	2.76
b1-3	-233.362704	0.053438	-233.309266	4.72	4.72
b1-4	-233.364045	0.053315	-233.310730	0.88	0.88
b1-5	-233.362915	0.053110	-233.309805	3.30	3.30
b1-6	-233.362921	0.053414	-233.309507	4.09	4.09
b1-7	-233.363746	0.053397	-233.310349	1.88	1.88
b1-8	-233.363049	0.053126	-233.309924	2.99	2.99
b1-9	-233.363205	0.053414	-233.309790	3.34	3.34
b2-1	-466.747567	0.113647	-466.633920	-30.96	-15.48
b2-2	-466.746523	0.113403	-466.633120	-28.86	-14.43
b2-3	-466.746260	0.112977	-466.633283	-29.29	-14.64
b2-4	-466.746061	0.113954	-466.632107	-26.20	-13.10
b2-5	-466.745747	0.113131	-466.632616	-27.54	-13.77
b2-6	-466.745513	0.113117	-466.632396	-26.96	-13.48
b2-7	-466.746194	0.114023	-466.632171	-26.37	-13.19
b2-8	-466.744801	0.113172	-466.631629	-24.95	-12.47
b2-9	-466.745212	0.113377	-466.631835	-25.49	-12.74
b3-1	-700.144217	0.179623	-699.964594	-82.45	-27.48
b3-2	-700.141608	0.178214	-699.963394	-79.30	-26.43
b3-3	-700.142303	0.178457	-699.963846	-80.49	-26.83
b3-4	-700.141499	0.177351	-699.964149	-81.28	-27.09
b3-5	-700.142047	0.177573	-699.964474	-82.13	-27.38
b3-6	-700.140717	0.177282	-699.963434	-79.40	-26.47
b3-7	-700.141081	0.177596	-699.963485	-79.54	-26.51
b3-8	-700.141601	0.178034	-699.963567	-79.75	-26.58
b3-9	-700.140015	0.177330	-699.962685	-77.44	-25.81
b3-10	-700.138384	0.176064	-699.962320	-76.48	-25.49
b4-1	-933.546440	0.245868	-933.300572	-147.86	-36.97
b4-2	-933.541957	0.244463	-933.297494	-139.78	-34.95
b4-3	-933.541867	0.243754	-933.298113	-141.40	-35.35
b4-4	-933.541773	0.243119	-933.298654	-142.83	-35.71
b4-5	-933.542254	0.244150	-933.298105	-141.38	-35.35
b4-6	-933.538713	0.242020	-933.296693	-137.68	-34.42
b4-7	-933.542638	0.243963	-933.298675	-142.88	-35.72
b4-8	-933.538406	0.243926	-933.294480	-131.87	-32.97
b4-9	-933.540366	0.244518	-933.295848	-135.46	-33.86
b5-1	-1166.942181	0.308889	-1166.633292	-204.72	-40.94
b5-2	-1166.936253	0.309433	-1166.626820	-187.73	-37.55
b5-3	-1166.926250	0.306273	-1166.619978	-169.76	-33.95
b6-1	-1400.336743	0.373245	-1399.963498	-254.98	-42.50
b6-2	-1400.333260	0.374458	-1399.958801	-242.65	-40.44
b6-3	-1400.326258	0.375843	-1399.950416	-220.63	-36.77
b6-6	-1400.301820	0.363636	-1399.938184	-188.52	-31.42

Table S13: Energies of the (R)-butan-2-ol clusters at the B3LYP/def2-TZVP level of theory. E_{elec} is the electronic energy, E_{gCP} is the geometrical counterpoise correction and E_{tot} is the sum of both, all three given in hartree. ΔE is the relative energy and $\Delta E/n$ is the relative energy divided by the number of molecules n contained in a cluster, both given in kJ mol^{-1}.

	B3LYP/def2-TZVP				
cluster	E_{elec}	E_{gCP}	E_{tot}	ΔE	$\Delta E/n$
b1-1	-233.633926	0.010627	-233.623300	0.36	0.36
b1-2	-233.633274	0.010660	-233.622614	2.16	2.16
b1-3	-233.632591	0.010745	-233.621846	4.17	4.17
b1-4	-233.634047	0.010611	-233.623436	0.00	0.00
b1-5	-233.633378	0.010657	-233.622720	1.88	1.88
b1-6	-233.632864	0.010679	-233.622186	3.28	3.28
b1-7	-233.634051	0.010701	-233.623350	0.22	0.22
b1-8	-233.633526	0.010668	-233.622859	1.51	1.51
b1-9	-233.633027	0.010681	-233.622346	2.86	2.86
b2-1	-467.280720	0.022436	-467.258284	-29.97	-14.98
b2-2	-467.279418	0.022402	-467.257016	-26.63	-13.32
b2-3	-467.279523	0.022336	-467.257186	-27.08	-13.54
b2-4	-467.279275	0.022544	-467.256730	-25.89	-12.94
b2-5	-467.279865	0.022372	-467.257493	-27.89	-13.94
b2-6	-467.279295	0.022450	-467.256845	-26.19	-13.09
b2-7	-467.278935	0.022574	-467.256361	-24.92	-12.46
b2-8	-467.278243	0.022389	-467.255855	-23.59	-11.79
b2-9	-467.278699	0.022481	-467.256218	-24.54	-12.27
b3-1	-700.937275	0.035326	-700.901949	-83.08	-27.69
b3-2	-700.935941	0.035175	-700.900766	-79.97	-26.66
b3-3	-700.936727	0.035079	-700.901647	-82.29	-27.43
b3-4	-700.936429	0.034976	-700.901453	-81.77	-27.26
b3-5	-700.936275	0.034935	-700.901340	-81.48	-27.16
b3-6	-700.935949	0.034984	-700.900964	-80.49	-26.83
b3-7	-700.935301	0.034939	-700.900363	-78.91	-26.30
b3-8	-700.934778	0.034891	-700.899888	-77.66	-25.89
b3-9	-700.934569	0.034966	-700.899603	-76.92	-25.64
b3-10	-700.932089	0.034588	-700.897501	-71.40	-23.80
b4-1	-934.598748	0.048238	-934.550510	-149.04	-37.26
b4-2	-934.596125	0.048028	-934.548097	-142.71	-35.68
b4-3	-934.595873	0.047971	-934.547902	-142.20	-35.55
b4-4	-934.596167	0.047681	-934.548486	-143.73	-35.93
b4-5	-934.596407	0.047946	-934.548461	-143.67	-35.92
b4-6	-934.594507	0.047701	-934.546806	-139.32	-34.83
b4-7	-934.596241	0.047891	-934.548350	-143.37	-35.84
b4-8	-934.593770	0.048114	-934.545656	-136.30	-34.07
b4-9	-934.594772	0.047985	-934.546787	-139.27	-34.82
b5-1	-1168.255808	0.060263	-1168.195545	-205.75	-41.15
b5-2	-1168.249519	0.060765	-1168.188755	-187.93	-37.59
b5-3	-1168.241823	0.060076	-1168.181747	-169.53	-33.91
b6-1	-1401.911613	0.072948	-1401.838665	-257.43	-42.91
b6-2	-1401.907037	0.073343	-1401.833694	-244.38	-40.73
b6-3	-1401.903397	0.074005	-1401.829392	-233.09	-38.85
b6-6	-1401.885806	0.071538	-1401.814268	-193.38	-32.23

Table S14: Energies of the mixed (R)-butan-2-ol acetonitrile clusters at the BP86/def2-SVP level of theory. E_{elec} is the electronic energy, E_{gCP} is the geometrical counterpoise correction and E_{tot} is the sum of both, all three given in hartree. ΔE is the relative energy and $\Delta E/n$ is the relative energy divided by the number of molecules n contained in a cluster, both given in $\mathrm{kJ\,mol^{-1}}$.

	BP86/def2-SVP				
cluster	E_{elec}	E_{gCP}	E_{tot}	ΔE	$\Delta E/n$
b1a1-1	-366.193249	0.071586	-366.121662	-20.37	-10.18
b1a1-2	-366.193257	0.071589	-366.121668	-20.38	-10.19
b1a1-3	-366.192507	0.072247	-366.120260	-16.69	-8.34
b1a2-1	-498.876357	0.090656	-498.785700	-62.86	-20.95
b1a2-2	-498.878019	0.091436	-498.786583	-65.18	-21.73
b1a2-3	-498.877277	0.091623	-498.785654	-62.74	-20.91
b1a3-1	-631.555567	0.110065	-631.445502	-94.23	-23.56
b1a3-2	-631.555096	0.111477	-631.443618	-89.29	-22.32
b1a3-3	-631.556762	0.111530	-631.445232	-93.52	-23.38
b1a4-1	-764.237188	0.129182	-764.108006	-132.70	-26.54
b1a4-2	-764.233661	0.130179	-764.103482	-120.82	-24.16
b1a4-3	-764.237261	0.129958	-764.107303	-130.85	-26.17
b1a5-1	-896.911328	0.150011	-896.761317	-147.03	-24.50
b1a5-2	-896.913648	0.148542	-896.765107	-156.98	-26.16
b1a5-3	-896.911149	0.149624	-896.761525	-147.57	-24.60
b2a1-1	-599.739667	0.133693	-599.605974	-68.32	-22.77
b2a1-2	-599.742585	0.134650	-599.607935	-73.46	-24.49
b2a1-3	-599.740864	0.134725	-599.606139	-68.75	-22.92
b2a2-1	-732.419974	0.153416	-732.266557	-101.74	-25.43
b2a2-2	-732.421342	0.153832	-732.267511	-104.24	-26.06
b2a2-3	-732.419628	0.155202	-732.264426	-96.14	-24.04
b2a2-4	-732.418226	0.150562	-732.267664	-104.64	-26.16
b2a3-1	-865.098747	0.172342	-864.926405	-133.23	-26.65
b2a3-2	-865.104627	0.173905	-864.930722	-144.56	-28.91
b2a3-3	-865.102882	0.173798	-864.929084	-140.26	-28.05
b2a3-4	-865.098002	0.172540	-864.925462	-130.75	-26.15
b2a4-1	-997.780665	0.193447	-997.587218	-167.25	-27.88
b2a4-2	-997.779115	0.194776	-997.584339	-159.70	-26.62
b2a4-3	-997.779135	0.194569	-997.584566	-160.29	-26.72
b3a1-1	-833.286031	0.195736	-833.090295	-116.29	-29.07
b3a1-2	-833.291280	0.198345	-833.092934	-123.21	-30.80
b3a1-3	-833.288380	0.197500	-833.090879	-117.82	-29.45
b3a2-1	-965.966901	0.216854	-965.750047	-147.53	-29.51
b3a2-2	-965.969751	0.219275	-965.750476	-148.65	-29.73
b3a2-3	-965.967318	0.218484	-965.748834	-144.34	-28.87
b3a3-1	-1098.643173	0.235749	-1098.407424	-172.53	-28.75
b3a3-2	-1098.648422	0.238625	-1098.409797	-178.76	-29.79
b3a3-3	-1098.645821	0.236848	-1098.408973	-176.60	-29.43
b3a3-4	-1098.632011	0.230144	-1098.401867	-157.94	-26.32
b4a1-1	-1066.831353	0.259313	-1066.572040	-157.49	-31.50
b4a1-2	-1066.839436	0.265934	-1066.573502	-161.33	-32.27
b4a1-3	-1066.836630	0.265559	-1066.571071	-154.95	-30.99
b4a2-1	-1199.514723	0.283868	-1199.230855	-186.27	-31.05
b4a2-2	-1199.519444	0.285730	-1199.233713	-193.78	-32.30
b4a2-3	-1199.520414	0.284464	-1199.235950	-199.65	-33.27
b5a1-1	-1300.390557	0.330089	-1300.060467	-216.24	-36.04
b5a1-2	-1300.390617	0.330078	-1300.060538	-216.43	-36.07
b5a1-3	-1300.387836	0.330602	-1300.057233	-207.75	-34.63

Table S15: Energies of the mixed (R)-butan-2-ol acetonitrile clusters at the BP86/def2-TZVP level of theory. E_{elec} is the electronic energy, E_{gCP} is the geometrical counterpoise correction and E_{tot} is the sum of both, all three given in hartree. ΔE is the relative energy and $\Delta E/n$ is the relative energy divided by the number of molecules n contained in a cluster, both given in kJ mol^{-1}.

	BP86/def2-TZVP				
cluster	E_{elec}	E_{gCP}	E_{tot}	ΔE	$\Delta E/n$
b1a1-1	-366.609318	0.013981	-366.595338	-20.61	-10.31
b1a1-2	-366.609335	0.013986	-366.595350	-20.65	-10.32
b1a1-3	-366.608388	0.014139	-366.594248	-17.75	-8.88
b1a2-1	-499.440243	0.017528	-499.422715	-59.01	-19.67
b1a2-2	-499.441510	0.017552	-499.423958	-62.28	-20.76
b1a2-3	-499.440852	0.017646	-499.423206	-60.30	-20.10
b1a3-1	-632.268504	0.021025	-632.247479	-90.55	-22.64
b1a3-2	-632.268574	0.021293	-632.247282	-90.03	-22.51
b1a3-3	-632.269089	0.021279	-632.247810	-91.42	-22.85
b1a4-1	-765.099025	0.024484	-765.074541	-128.12	-25.62
b1a4-2	-765.096724	0.024673	-765.072051	-121.58	-24.32
b1a4-3	-765.098970	0.024637	-765.074333	-127.57	-25.51
b1a5-1	-897.924842	0.028444	-897.896398	-152.02	-25.34
b1a5-2	-897.924730	0.028140	-897.896590	-152.52	-25.42
b1a5-3	-897.923577	0.028359	-897.895219	-148.92	-24.82
b2a1-1	-600.414802	0.026084	-600.388718	-69.57	-23.19
b2a1-2	-600.416957	0.026192	-600.390765	-74.95	-24.98
b2a1-3	-600.414719	0.026475	-600.388244	-68.33	-22.78
b2a2-1	-733.243853	0.029757	-733.214096	-102.72	-25.68
b2a2-2	-733.245036	0.029710	-733.215326	-105.95	-26.49
b2a2-3	-733.243199	0.030092	-733.213107	-100.12	-25.03
b2a2-4	-733.242266	0.029319	-733.212948	-99.70	-24.93
b2a3-1	-866.072708	0.033376	-866.039332	-135.49	-27.10
b2a3-2	-866.076267	0.033329	-866.042938	-144.96	-28.99
b2a3-3	-866.074702	0.033367	-866.041335	-140.75	-28.15
b2a3-4	-866.070925	0.033289	-866.037636	-131.04	-26.21
b2a4-1	-998.902148	0.037051	-998.865097	-169.66	-28.28
b2a4-2	-998.901353	0.037354	-998.863999	-166.78	-27.80
b2a4-3	-998.900871	0.037334	-998.863537	-165.56	-27.59
b3a1-1	-834.221333	0.038565	-834.182768	-120.29	-30.07
b3a1-2	-834.224948	0.038407	-834.186540	-130.19	-32.55
b3a1-3	-834.221542	0.038609	-834.182933	-120.72	-30.18
b3a2-1	-967.050556	0.042187	-967.008369	-154.02	-30.80
b3a2-2	-967.051767	0.042520	-967.009247	-156.32	-31.26
b3a2-3	-967.049273	0.042656	-967.006617	-149.42	-29.88
b3a3-1	-1099.876439	0.045676	-1099.830763	-179.33	-29.89
b3a3-2	-1099.879264	0.046254	-1099.833010	-185.23	-30.87
b3a3-3	-1099.877461	0.045772	-1099.831690	-181.77	-30.29
b3a3-4	-1099.868934	0.045076	-1099.823858	-161.21	-26.87
b4a1-1	-1068.026600	0.050820	-1067.975780	-168.28	-33.66
b4a1-2	-1068.030026	0.052047	-1067.977979	-174.05	-34.81
b4a1-3	-1068.027849	0.051840	-1067.976009	-168.88	-33.78
b4a2-1	-1200.856310	0.055274	-1200.801036	-201.11	-33.52
b4a2-2	-1200.859067	0.055771	-1200.803296	-207.04	-34.51
b4a2-3	-1200.859988	0.055545	-1200.804442	-210.05	-35.01
b5a1-1	-1301.839518	0.064402	-1301.775116	-232.87	-38.81
b5a1-2	-1301.839550	0.064404	-1301.775146	-232.95	-38.82
b5a1-3	-1301.836168	0.064912	-1301.771256	-222.74	-37.12

Table S16: Energies of the mixed (R)-butan-2-ol acetonitrile clusters at the B3LYP/def2-SVP level of theory. E_{elec} is the electronic energy, E_{gCP} is the geometrical counterpoise correction and E_{tot} is the sum of both, all three given in hartree. ΔE is the relative energy and $\Delta E/n$ is the relative energy divided by the number of molecules n contained in a cluster, both given in kJ mol^{-1}.

	B3LYP/def2-SVP				
cluster	E_{elec}	E_{gCP}	E_{tot}	ΔE	$\Delta E/n$
b1a1-1	-365.954971	0.072273	-365.882698	-21.92	-10.96
b1a1-2	-365.954978	0.072274	-365.882703	-21.93	-10.97
b1a1-3	-365.954468	0.072899	-365.881569	-18.95	-9.48
b1a2-1	-498.553734	0.091168	-498.462566	-65.45	-21.82
b1a2-2	-498.555592	0.091824	-498.463768	-68.61	-22.87
b1a2-3	-498.554788	0.091993	-498.462795	-66.05	-22.02
b1a3-1	-631.149483	0.110563	-631.038919	-99.76	-24.94
b1a3-2	-631.149022	0.111839	-631.037183	-95.20	-23.80
b1a3-3	-631.150618	0.111969	-631.038649	-99.05	-24.76
b1a4-1	-763.747457	0.129567	-763.617890	-140.94	-28.19
b1a4-2	-763.744534	0.130768	-763.613767	-130.12	-26.02
b1a4-3	-763.747588	0.130360	-763.617228	-139.20	-27.84
b1a5-1	-896.338886	0.150534	-896.188351	-159.78	-26.63
b1a5-2	-896.340720	0.148944	-896.191776	-168.77	-28.13
b1a5-3	-896.338436	0.149980	-896.188456	-160.05	-26.68
b2a1-1	-599.347155	0.134365	-599.212790	-71.88	-23.96
b2a1-2	-599.350343	0.135262	-599.215080	-77.89	-25.96
b2a1-3	-599.348523	0.135299	-599.213225	-73.02	-24.34
b2a2-1	-731.943689	0.154157	-731.789533	-107.21	-26.80
b2a2-2	-731.945576	0.154456	-731.791120	-111.38	-27.84
b2a2-3	-731.943525	0.155725	-731.787800	-102.66	-25.66
b2a2-4	-731.941499	0.151278	-731.790221	-109.01	-27.25
b2a3-1	-864.538564	0.172971	-864.365594	-140.75	-28.15
b2a3-2	-864.544573	0.174451	-864.370122	-152.64	-30.53
b2a3-3	-864.542617	0.174616	-864.368001	-147.07	-29.41
b2a3-4	-864.538223	0.173138	-864.365085	-139.41	-27.88
b2a4-1	-997.136810	0.193959	-996.942851	-177.43	-29.57
b2a4-2	-997.136227	0.195170	-996.941057	-172.72	-28.79
b2a4-3	-997.136516	0.195139	-996.941376	-173.56	-28.93
b3a1-1	-832.738650	0.196269	-832.542382	-120.52	-30.13
b3a1-2	-832.744736	0.198500	-832.546237	-130.64	-32.66
b3a1-3	-832.741763	0.198217	-832.543546	-123.58	-30.89
b3a2-1	-965.336614	0.217289	-965.119325	-156.38	-31.28
b3a2-2	-965.340472	0.219862	-965.120610	-159.75	-31.95
b3a2-3	-965.338433	0.219123	-965.119311	-156.34	-31.27
b3a3-1	-1097.929254	0.236250	-1097.693005	-183.67	-30.61
b3a3-2	-1097.935722	0.239527	-1097.696194	-192.04	-32.01
b3a3-3	-1097.932132	0.237466	-1097.694666	-188.03	-31.34
b3a3-4	-1097.919877	0.231889	-1097.687988	-170.50	-28.42
b4a1-1	-1066.130526	0.259155	-1065.871370	-167.58	-33.52
b4a1-2	-1066.139778	0.265897	-1065.873881	-174.18	-34.84
b4a1-3	-1066.136260	0.265919	-1065.870341	-164.88	-32.98
b4a2-1	-1198.729758	0.284342	-1198.445416	-195.83	-32.64
b4a2-2	-1198.736392	0.286166	-1198.450226	-208.46	-34.74
b4a2-3	-1198.735287	0.284826	-1198.450461	-209.08	-34.85
b5a1-1	-1299.536717	0.330308	-1299.206409	-230.53	-38.42
b5a1-2	-1299.536723	0.330329	-1299.206394	-230.49	-38.42
b5a1-3	-1299.533022	0.330921	-1299.202100	-219.22	-36.54

Table S17: Energies of the mixed (R)-butan-2-ol acetonitrile clusters at the B3LYP/def2-TZVP level of theory. E_{elec} is the electronic energy, E_{gCP} is the geometrical counterpoise correction and E_{tot} is the sum of both, all three given in hartree. ΔE is the relative energy and $\Delta E/n$ is the relative energy divided by the number of molecules n contained in a cluster, both given in kJ mol^{-1}.

	B3LYP/def2-TZVP				
cluster	E_{elec}	E_{gCP}	E_{tot}	ΔE	$\Delta E/n$
b1a1-1	-366.376753	0.014143	-366.362610	-21.47	-10.74
b1a1-2	-366.376765	0.014145	-366.362619	-21.50	-10.75
b1a1-3	-366.375897	0.014285	-366.361612	-18.85	-9.43
b1a2-1	-499.126063	0.017647	-499.108416	-60.00	-20.00
b1a2-2	-499.127482	0.017667	-499.109814	-63.67	-21.22
b1a2-3	-499.126764	0.017750	-499.109013	-61.56	-20.52
b1a3-1	-631.873744	0.021359	-631.852385	-93.70	-23.42
b1a3-2	-631.873467	0.021374	-631.852093	-92.93	-23.23
b1a3-3	-631.873957	0.021401	-631.852556	-94.15	-23.54
b1a4-1	-764.622898	0.024625	-764.598273	-132.44	-26.49
b1a4-2	-764.621027	0.024815	-764.596212	-127.03	-25.41
b1a4-3	-764.622813	0.024771	-764.598042	-131.83	-26.37
b1a5-1	-897.368305	0.028554	-897.339751	-159.60	-26.60
b1a5-2	-897.367899	0.028271	-897.339628	-159.28	-26.55
b1a5-3	-897.366865	0.028466	-897.338399	-156.05	-26.01
b2a1-1	-600.030727	0.026241	-600.004486	-70.24	-23.41
b2a1-2	-600.032975	0.026325	-600.006650	-75.92	-25.31
b2a1-3	-600.030648	0.026593	-600.004055	-69.11	-23.04
b2a2-1	-732.778577	0.029919	-732.748658	-104.48	-26.12
b2a2-2	-732.780243	0.029871	-732.750372	-108.98	-27.24
b2a2-3	-732.778011	0.030200	-732.747812	-102.26	-25.56
b2a2-4	-732.777107	0.029483	-732.747625	-101.77	-25.44
b2a3-1	-865.526305	0.033518	-865.492787	-138.60	-27.72
b2a3-2	-865.529778	0.033475	-865.496302	-147.83	-29.57
b2a3-3	-865.528097	0.033524	-865.494573	-143.29	-28.66
b2a3-4	-865.524749	0.033412	-865.491337	-134.79	-26.96
b2a4-1	-998.274510	0.037192	-998.237318	-173.78	-28.96
b2a4-2	-998.274285	0.037413	-998.236872	-172.61	-28.77
b2a4-3	-998.273941	0.037457	-998.236484	-171.59	-28.60
b3a1-1	-833.685328	0.038635	-833.646693	-119.88	-29.97
b3a1-2	-833.689253	0.038604	-833.650649	-130.27	-32.57
b3a1-3	-833.686001	0.038748	-833.647253	-121.35	-30.34
b3a2-1	-966.433643	0.042295	-966.391348	-155.39	-31.08
b3a2-2	-966.435559	0.042633	-966.392926	-159.53	-31.91
b3a2-3	-966.433379	0.042695	-966.390684	-153.64	-30.73
b3a3-1	-1099.178897	0.045764	-1099.133133	-183.36	-30.56
b3a3-2	-1099.182570	0.046407	-1099.136163	-191.31	-31.89
b3a3-3	-1099.179929	0.045910	-1099.134019	-185.68	-30.95
b3a3-4	-1099.171593	0.045194	-1099.126399	-165.68	-27.61
b4a1-1	-1067.339217	0.050892	-1067.288324	-168.01	-33.60
b4a1-2	-1067.343631	0.052040	-1067.291592	-176.59	-35.32
b4a1-3	-1067.340696	0.051968	-1067.288728	-169.07	-33.81
b4a2-1	-1200.087422	0.055243	-1200.032179	-201.42	-33.57
b4a2-2	-1200.091700	0.055806	-1200.035894	-211.17	-35.19
b4a2-3	-1200.091154	0.055584	-1200.035569	-210.32	-35.05
b5a1-1	-1301.001467	0.064318	-1300.937149	-235.03	-39.17
b5a1-2	-1301.001473	0.064325	-1300.937148	-235.03	-39.17
b5a1-3	-1300.997412	0.064811	-1300.932601	-223.09	-37.18

References

(1) Weinhold, F. Quantum cluster equilibrium theory of liquids: General theory and computer implementation. *J. Chem. Phys.* **1998**, *109*, 367–372.

(2) Kirchner, B. Cooperative versus dispersion effects: What is more important in an associated liquid such as water? *J. Chem. Phys.* **2005**, *123*, 204116.

(3) Chai, J.-D.; Head-Gordon, M. Long-range corrected hybrid density functionals with damped atom–atom dispersion corrections. *Phys. Chem. Chem. Phys.* **2008**, *10*, 6615–6620.

(4) Brüssel, M.; Perlt, E.; Lehmann, S. B.; von Domaros, M.; Kirchner, B. Binary systems from quantum cluster equilibrium theory. *J. Chem. Phys.* **2011**, *135*, 194113.

(5) Kirchner, B.; Spickermann, C.; Lehmann, S. B.; Perlt, E.; Langner, J.; von Domaros, M.; Reuther, P.; Uhlig, F.; Kohagen, M.; Brüssel, M. What can clusters tell us about the bulk?: Peacemaker: Extended quantum cluster equilibrium calculations. *Comput. Phys. Commun.* **2011**, *182*, 1428–1446.

(6) von Domaros, M.; Perlt, E.; Ingenmey, J.; Marchelli, G.; Kirchner, B. Peacemaker 2: Making clusters talk about binary mixtures and neat liquids. *SoftwareX* **2018**, *7*, 356–359.

(7) McQuarrie, D. A.; Simon, J. D. *Physical chemistry: a molecular approach, vol. 1*; University Science Books: USA, 1997.

(8) Wedler, G.; Freund, H.-J. *Lehrbuch der physikalischen Chemie*; John Wiley & Sons, 2012; Vol. 1.

(9) Marchelli, G.; Ingenmey, J.; Hollóczki, O.; Chaumont, A.; Kirchner, B. Hydrogen Bonding and Vaporization Thermodynamics in Hexafluoroisopropanol-Acetone

and-Methanol Mixtures. A Joined Cluster Analysis and Molecular Dynamic Study. *ChemPhysChem* **2022**, *23*, 50–62.

(10) Zaby, P.; Ingenmey, J.; Kirchner, B.; Grimme, S.; Ehlert, S. Calculation of improved enthalpy and entropy of vaporization by a modified partition function in quantum cluster equilibrium theory. *J. Chem. Phys.* **2021**, *155*, 104101.

(11) Grimme, S. Supramolecular binding thermodynamics by dispersion-corrected density functional theory. *Chem. Eur. J.* **2012**, *18*, 9955–9964.

(12) Ingenmey, J.; Blasius, J.; Marchelli, G.; Riegel, A.; Kirchner, B. A Cluster Approach for Activity Coefficients: General Theory and Implementation. *J. Chem. Eng. Data* **2019**, *64*, 255–261.

(13) Blasius, J.; Kirchner, B. Cluster-weighting in bulk phase vibrational circular dichroism. *J. Phys. Chem. B* **2020**, *124*, 7272–7283.

(14) Dieterich, J. M.; Hartke, B. OGOLEM: global cluster structure optimisation for arbitrary mixtures of flexible molecules. A multiscaling, object-oriented approach. *Mol. Phys.* **2010**, *108*, 279–291.

(15) Dieterich, J. M.; Hartke, B. Composition-induced structural transitions in mixed Lennard-Jones clusters: Global reparametrization and optimization. *J. Comput. Chem.* **2011**, *32*, 1377–1385.

(16) Case, D. A.; Betz, R. M.; Cerutti, D. S.; Cheatham, T. E.; Darden, T. A.; Duke, R. E.; Giese, T. J.; Gohlke, H.; Goetz, A. W.; Homeyer, N.; et al., AMBER 2016 (University of California). *San Francisco* **2016**,

(17) Wang, J.; Wolf, R. M.; Caldwell, J. W.; Kollman, P. A.; Case, D. A. Development and testing of a general amber force field. *J. Comput. Chem.* **2004**, *25*, 1157–1174.

(18) Ahlrichs, R.; Bär, M.; Häser, M.; Horn, H.; Kölmel, C. Electronic structure calculations on workstation computers: The program system turbomole. *Chem. Phys. Lett.* **1989**, *162*, 165–169.

(19) Reiter, K.; Kühn, M.; Weigend, F. Vibrational circular dichroism spectra for large molecules and molecules with heavy elements. *J. Chem. Phys.* **2017**, *146*, 054102.

(20) Balasubramani, S. G.; Chen, G. P.; Coriani, S.; Diedenhofen, M.; Frank, M. S.; Franzke, Y. J.; Furche, F.; Grotjahn, R.; Harding, M. E.; Hättig, C.; et al., TURBOMOLE: Modular program suite for ab initio quantum-chemical and condensed-matter simulations. *J. Chem. Phys.* **2020**, *152*, 184107.

(21) TURBOMOLE V7.5 2020, a development of University of Karlsruhe and Forschungszentrum Karlsruhe GmbH, 1989-2007, TURBOMOLE GmbH, since 2007; available from
`https://www.turbomole.org`.

(22) Becke, A. D. Density-functional exchange-energy approximation with correct asymptotic behavior. *Phys. Rev. A* **1988**, *38*, 3098–3100.

(23) Perdew, J. P. Density-functional approximation for the correlation energy of the inhomogeneous electron gas. *Phys. Rev. B* **1986**, *33*, 8822–8824.

(24) Weigend, F.; Ahlrichs, R. Balanced basis sets of split valence, triple zeta valence and quadruple zeta valence quality for H to Rn: Design and assessment of accuracy. *Phys. Chem. Chem. Phys.* **2005**, *7*, 3297–3305.

(25) Grimme, S.; Antony, J.; Ehrlich, S.; Krieg, H. A consistent and accurate ab initio parametrization of density functional dispersion correction (DFT-D) for the 94 elements H-Pu. *J. Chem. Phys.* **2010**, *132*, 154104.

(26) Grimme, S.; Ehrlich, S.; Goerigk, L. Effect of the damping function in dispersion corrected density functional theory. *J. Comput. Chem.* **2011**, *32*, 1456–1465.

(27) Kruse, H.; Grimme, S. A geometrical correction for the inter-and intra-molecular basis set superposition error in Hartree-Fock and density functional theory calculations for large systems. *J. Chem. Phys.* **2012**, *136*, 154101.

(28) Kirchner, B.; Blasius, J.; Esser, L.; Reckien, W. Predicting Vibrational Spectroscopy for Flexible Molecules and Molecules with Non-Idle Environments. *Adv. Theory Simul.* **2021**, *4*, 2000223.

(29) Bondi, A. v. van der Waals volumes and radii. *J. Phys. Chem.* **1964**, *68*, 441–451.

(30) Taherivardanjani, S.; Blasius, J.; Brehm, M.; Dötzer, R.; Kirchner, B. Conformer Weighting and Differently Sized Cluster Weighting for Nicotine and Its Phosphorus Derivatives. *J. Phys. Chem. A* **2022**,

(31) Storn, R.; Price, K. Differential evolution–a simple and efficient heuristic for global optimization over continuous spaces. *J. Glob. Optim.* **1997**, *11*, 341–359.

(32) Virtanen, P.; Gommers, R.; Oliphant, T. E.; Haberland, M.; Reddy, T.; Cournapeau, D.; Burovski, E.; Peterson, P.; Weckesser, W.; Bright, J., et al. SciPy 1.0: fundamental algorithms for scientific computing in Python. *Nat. Methods* **2020**, *17*, 261–272.

(33) Mathieu, D.; Defranceschi, M.; Delhalle, J. Ab initio study of the influence of aggregation on the infrared spectrum of acetonitrile. *Int. J. Quantum Chem.* **1993**, *45*, 735–746.

(34) Pace, E.; Noe, L. J. Infrared Spectra of Acetonitrile and Acetonitrile-d3. *J. Chem. Phys.* **1968**, *49*, 5317–5325.

(35) Galabov, B.; Yamaguchi, Y.; Remington, R. B.; Schaefer, H. F. High level ab initio quantum mechanical predictions of infrared intensities. *J. Phys. Chem. A* **2002**, *106*, 819–832.

(36) Shen, J.; Zhu, C.; Reiling, S.; Vaz, R. A novel computational method for comparing vibrational circular dichroism spectra. *Spectrochim. Acta Part A: Mol. Biomol. Spectrosc.* **2010**, *76*, 418–422.

(37) Wang, F.; Polavarapu, P. L. Vibrational circular dichroism: Predominant conformations and intermolecular interactions in (R)-(-)-2-butanol. *J. Phys. Chem. A* **2000**, *104*, 10683–10687.

(38) Thomas, M.; Kirchner, B. Classical magnetic dipole moments for the simulation of vibrational circular dichroism by ab initio molecular dynamics. *J. Phys. Chem. Lett.* **2016**, *7*, 509–513.